Stabilizing Quantum Gravity: A Recoverable Quantum-Code Framework for Spacetime, Gauge Structure, and Matter

George Mallis

April 28, 2026

Abstract

We present Stabilizing Quantum Gravity (SQG), a recoverability-based operator-algebraic and quantum-information framework in which effective spacetime geometry, gravitational response, gauge structure, and matter-like sectors arise from a finite-depth logical substrate endowed with stabilizer organization. Rather than quantizing a pre-given metric or inserting gauge symmetries and matter fields as primitive microscopic inputs, SQG treats them as emergent consequences of which logical sectors remain recoverable, stable, and dynamically admissible.

At the structural level developed here, the framework is built on three central ingredients: a net of recoverable operator-algebra sectors, finite logical depth, and a stabilization principle selecting persistent phases under admissible deformations. On this basis, the manuscript develops the core backbone of the SQG program. First, it establishes a logical composition ceiling: under multiplicative norm preservation, nondegeneracy, and finite recoverability depth, admissible finite-dimensional logical composition sectors are restricted by a Hurwitz-type bound. Second, it develops the recoverability-to-Einstein bridge, in which modular structure, generalized entropy extremality, and recoverability jointly generate an effective semiclassical gravitational response, with the Einstein limit recovered in saturated regimes. Third, it organizes gauge symmetry, matter, and chirality into a unified code-theoretic architecture: gauge symmetry is interpreted as stabilizer redundancy, matter as persistent localized defect structure, and chirality as a protected bulk–defect/interface asymmetry problem rather than a primitive microscopic input.

The purpose of the present paper is not to claim that every branch of this program is already complete at the same level. Its purpose is sharper: to establish the strongest current common structural spine of SQG and to distinguish clearly between results that are already closed at theorem level, sectors that admit conditional closure under stated hypotheses, and frontier modules whose remaining constructive bottlenecks are now explicit.

Phenomenologically, SQG yields a constrained modification pattern: departures from General Relativity are confined to a scalar/environmental response channel, while tensor propagation remains symmetry-protected, luminal, and polarization-stable. In this way, the framework recovers local QFT+GR behavior in stabilized phases while opening a mathematically controlled route toward ultraviolet consistency, defect matter sectors, protected chirality, horizon thermodynamics, black-hole information recovery, and large-scale unsaturated cosmological response.

The resulting picture is ambitious but disciplined: spacetime, matter, gauge redundancy, and information-theoretic gravitational response are treated not as disconnected primitives, but as linked manifestations of one recoverable logical architecture.

Contents

1 Introduction

The Stabilizing Quantum Gravity (SQG) program begins from a sharper premise than that of most unification attempts: spacetime geometry, gauge structure, and matter are not taken as primitive ingredients to be quantized, decorated, or patched together, but as effective manifestations of a deeper recoverable logical substrate. In SQG, the fundamental layer is not a pre-given metric manifold, nor a bare collection of elementary fields, but a stabilizer-organized operator-algebraic architecture whose persistent sectors define what low-energy observers interpret as geometry, interaction structure, and localized matter content.

This shift is more than philosophical packaging. It changes the order of explanation. In conventional approaches, one usually starts with geometry, gauge symmetry, and matter, and then asks how to quantize or unify them. In SQG, one begins instead with recoverability, finite logical depth, stabilizer organization, and admissible defect structure, and asks which large-scale sectors survive as dynamically stable, reconstructible, and physically meaningful. Geometry then appears not as a primitive background, but as a stabilized phase; gauge symmetry not as a microscopic axiom, but as logical redundancy; and matter not as an external input, but as persistent localized defect structure inside an otherwise recoverable substrate.

Within this architecture, the K2 and K3 sectors capture two decisive layers of emergence. First, recoverable informational organization gives rise to effective spacetime structure and semiclassical gravitational response. Second, localized failures of perfect stabilizer recovery define defect sectors that act as matter-like excitations. These two layers already suggest a unification principle stronger than mere coexistence: geometry and matter are not independent starting ingredients, but different organized regimes of the same deeper logical medium.

A realistic foundational theory, however, must explain more than the appearance of geometry and localized excitations. It must also account for the strikingly constrained interaction architecture observed in nature. The Standard Model is not merely a list of particles; it is a rigid gauge-theoretic structure built around

$$SU(3) \times SU(2) \times U(1),$$

together with highly nontrivial restrictions on charge assignment, chirality, anomaly cancellation, and admissible local organization. In most bottom-up formulations this structure is simply assumed. In SQG the question is more severe: can such gauge structure arise because recoverable logical organization permits only a narrow class of continuous redundancies to survive?

The present paper develops precisely that possibility. Its central claim is that gauge symmetry should be interpreted as stabilizer redundancy of admissible logical sectors, and that the same recoverability and finite-depth conditions which stabilize the emergent geometric phase also sharply constrain the local continuous symmetry structure acting on that phase. This brings gauge emergence into direct contact with the algebraic limits of norm-preserving logical composition.

The key structural result is the logical composition ceiling associated with multiplicative norm preservation and finite recoverability depth. Combined with the Hurwitz classification of real normed composition algebras, this ceiling severely restricts the admissible local algebraic structure of persistent sectors. The significance of this restriction is not merely algebraic. It compresses the space of viable emergent interaction architectures. The resulting picture is not yet a full derivation of all Standard Model phenomenology, but it is already strong enough to make the observed narrowness of gauge structure look increasingly structural rather than accidental.

In that sense, the role of the present work is not to declare a finished Theory of Everything, but to establish a common theorem-oriented backbone on which its major sectors can be judged honestly: some already theorem-level closed, some conditionally closed under explicit hypotheses, and some now reduced to sharply defined constructive bottlenecks rather than vague promises. That distinction is crucial. A framework becomes scientifically stronger not when it claims everything at once, but when it makes precise which parts are already rigid, which are conditional, and exactly where the remaining burden lies. In this sense, the role of the present paper is not to postulate gauge symmetry, but to explain why only a narrow class of continuous redundancies can consistently survive inside a recoverable substrate.

Program Architecture

The present manuscript should be read as the structural backbone of the broader SQG research program. Its purpose is not to force every branch of the theory to the same level of completion, but to establish the common recoverability-based architecture from which its major physical sectors arise.

- **Recoverability backbone:** a recoverable operator-algebraic substrate, finite-depth logical admissibility, and a stabilization principle selecting persistent sectors under admissible deformations.
- **Logical composition ceiling:** multiplicative norm preservation in the recoverable logical layer enforces a Hurwitz-type bound on admissible local algebraic structure, sharply restricting the space of consistent sectors.
- **Einstein bridge:** recoverable informational balance and modular structure generate an Einstein-type gravitational response, providing the core route from recoverability to emergent semiclassical geometry.
- **Gauge emergence:** local gauge symmetry is interpreted not as a primitive axiom but as stabilizer redundancy of maximally admissible logical organization.
- **Matter from defects:** matter is not treated as primitive ontology, but as persistent localized defect structure - the structured scar of imperfect recoverability inside an otherwise stabilized substrate.
- **Chirality branch:** chirality is elevated from a loose phenomenological requirement to a protected bulk-defect interface problem with an explicit theorem-program route and constructive closure targets.
- **Large-scale and extreme-sector extensions:** the same framework extends toward horizon stabilization phases, black-hole information recovery, cosmological recovery–defect dynamics, and dimensional or logical sector selection.
- **Claim hierarchy:** the present manuscript establishes the strongest current structural spine of SQG, while the associated matter, chirality, horizon, and cosmological sectors are developed with different levels of theorem-level closure, explicit construction, and phenomenological completion.
- **Broader outlook:** the recoverability architecture may also support more distant observer-related foundational extensions, although such questions lie outside the scope of the present submission.

2 Quantum Information-Theoretic Foundations

2.1 Quantum Logical Substrate

The logical algebra $\mathcal{A}_{log}$ is interpreted as the observable algebra of a finite-depth quantum code. States on $\mathcal{A}_{log}$ are density operators on a Hilbert space $\mathcal{H}_{code}$.

Recoverability is identified with approximate quantum error correction in the sense of operator-algebraic quantum codes.

2.2 Categorical Admissibility and Microscopic Realizability

The algebraic SQG framework is intentionally substrate-independent. However, not every abstract logical algebra should be regarded as physically admissible. We therefore refine the notion of an admissible sector by requiring compatibility with protected categorical data.

Definition 2.1 (Categorically admissible sector)**.** A logical sector $\mathcal{A}_{\log}$ is called categorically admissible if there exists a unitary fusion category, braided fusion category, or higher-categorical extension $\mathcal{C}$ such that:

1. the protected defect data of $\mathcal{C}$ admit a faithful realization of $\mathcal{A}_{\log}$,
2. the sector is compatible with finite recoverability depth,
3. tensor-sector protection is preserved,
4. no anomaly obstructs the existence of a consistent infrared effective sector.

Interpretation. This requirement excludes arbitrary algebraic constructions with no protected microscopic completion. It also provides the natural bridge from the abstract SQG framework to string-net, quantum-double, and modular-tensor realizations.

Functorial emergence principle. When such a category exists, we may regard effective bulk operators as images of protected topological data under a decoding functor

$$D : Z(\mathcal{C}) \longrightarrow \mathrm{QFT}_{\mathrm{eff}}^{3+1}, \qquad D(X, c_{X,-}) \mapsto \Phi_X(x), \tag{1}$$

where $Z(\mathcal{C})$ denotes the Drinfeld center. This does not make geometry fundamental; it states only that admissible bulk degrees of freedom must descend from protected microscopic sectors.

Scope. The present paper uses this principle as a structural admissibility condition, not as a full matter-from-code derivation. Gauge structure, chirality, and family replication are deferred to sequel papers.

2.3 Stabilizer Structure

We assume the existence of a stabilizer subgroup $\mathcal{S} \subset \mathcal{A}_{log}$ such that physical states satisfy:

$$S|\psi\rangle = |\psi\rangle \quad \forall S \in \mathcal{S}. \tag{2}$$

In the operator-algebraic language used later, stabilizer constraints are implemented via conditional expectations onto code-preserving subalgebras, and the Hilbert-space notation is used as an equivalent concrete representation when a code subspace is fixed.

Logical operators act on the code subspace:

$$\mathcal{H}_{phys} = \{|\psi\rangle \in \mathcal{H}_{code} \mid S|\psi\rangle = |\psi\rangle\}. \tag{3}$$

2.4 Logical Depth as Circuit Complexity

Finite logical depth corresponds to bounded quantum circuit complexity:

$$d < \infty \quad \Longleftrightarrow \quad \text{finite quantum circuit preparation.} \tag{4}$$

Thus SQG is fundamentally a finite-depth quantum error-correcting code whose low-energy excitations generate geometry and matter.

2.5 Minimal Stability Bound and the Necessity of Fault Tolerance

Toy model. Consider a finite-depth stabilizer architecture subject to an effective local error rate $p \in [0, 1]$ per depth layer. Let p_{th} denote a threshold such that for $p < p_{\text{th}}$ recovery succeeds with nonzero asymptotic fidelity, while for $p > p_{\text{th}}$ logical information delocalizes.

Assumption 2.2 (Threshold property (toy))**.** *There exists $p_{\text{th}} \in (0, 1)$ and constants $c, \alpha > 0$ such that for depth d,*

$$p < p_{\text{th}} \Rightarrow 1 - F_{\text{rec}}(d) \leq c\, e^{-\alpha d}, \qquad p > p_{\text{th}} \Rightarrow F_{\text{rec}}(d) \to 0 \text{ as } d \to \infty.$$

Theorem 2.3 (Lower bound on stable sector persistence (toy))**.** *Under Assumption 2.2, any emergent semiclassical sector requiring recoverability fidelity $F_{\text{rec}} \geq 1 - \varepsilon$ must satisfy*

$$d \;\geq\; \frac{1}{\alpha} \log\!\left(\frac{c}{\varepsilon}\right) \quad \text{whenever } p < p_{\text{th}}.$$

Sketch. Immediate from $1 - F_{\text{rec}}(d) \leq ce^{-\alpha d}$ by solving for d given ε. □

Remark 2.4 (Interpretation). This toy bound formalizes the statement: *a persistent semiclassical world requires fault-tolerant stabilization.* The threshold and scaling are to be derived from explicit code families and noise models; the present statement is a structurally motivated constraint.

3 Emergent Gauge Structure and the Standard Model Factor

3.1 Stabilizer Redundancy and Gauge Automorphisms

Let $\mathcal{A}_{log}$ be the logical operator algebra acting on a code Hilbert space $\mathcal{H}_{code}$ with stabilizer subgroup $\mathcal{S} \subset \mathcal{A}_{log}$. Define the *gauge-acting automorphisms* as the subgroup

$$\text{Aut}_{\mathcal{S}}(\mathcal{A}_{log}) := \{\alpha \in \text{Aut}(\mathcal{A}_{log}) \mid \alpha(\mathcal{S}) = \mathcal{S}\}. \tag{5}$$

Trivial (stabilizer-equivalent) actions are given by inner automorphisms generated by stabilizers,

$$\text{Inn}_{\mathcal{S}} := \{\text{Ad}_U(\cdot) = U(\cdot)U^\dagger \mid U \in \langle \mathcal{S} \rangle\}. \tag{6}$$

We define the emergent gauge group by the quotient

$$\mathcal{G}_{gauge} := \mathrm{Aut}_{\mathcal{S}}(\mathcal{A}_{log}) \,/\, \mathrm{Inn}_{\mathcal{S}}. \tag{7}$$

3.2 Gauge Coupling Unification from Stabilizer Density

In SQG, gauge kinetic terms arise from stabilizer fluctuation response. The Yang–Mills action takes the form:

$$S_{YM} = \int d^4x \sqrt{-g} \sum_i \frac{\kappa_i \rho_{stab}}{4} \mathrm{Tr}(F^{(i)}_{\mu\nu} F^{(i)\mu\nu}), \tag{8}$$

where ρ_{stab} is the universal stabilizer density and κ_i are group-theoretic normalization constants.

Identifying:

$$\frac{1}{g_i^2} = \kappa_i \rho_{stab}, \tag{9}$$

we obtain:

$$g_i^2 = \frac{1}{\kappa_i \rho_{stab}}. \tag{10}$$

If ρ_{stab} is universal at a stabilization scale Λ_{stab} (Assumption U1), then the couplings satisfy a common boundary condition up to group normalizations:

Assumption 3.1 (U1: Universality of stabilizer density at Λ_{stab})**.** *At the stabilization scale, ρ_{stab} is sector-independent within the visible gauge bundle.*

Λ_{stab}, then couplings unify up to normalization factors:

$$\frac{g_1^2}{\kappa_1} = \frac{g_2^2}{\kappa_2} = \frac{g_3^2}{\kappa_3}. \tag{11}$$

Choosing canonical normalization consistent with embedding into a simple algebra yields:

$$g_1 = g_2 = g_3 \quad \text{at} \quad \Lambda_{stab}. \tag{12}$$

Below Λ_{stab}, renormalization group flow induces splitting consistent with Standard Model running.

3.3 Weinberg Angle at Stabilization Scale (Target Relation)

Canonical normalization of the $U(1)_Y$ generator consistent with embedding into a simple compact algebra yields:

$$g_1^2 = \frac{5}{3} g_Y^2. \tag{13}$$

Unification condition at Λ_{stab}:

$$g_1 = g_2 = g_3. \tag{14}$$

This implies:

$$\sin^2\theta_W(\Lambda_{stab}) = \frac{g_Y^2}{g_2^2 + g_Y^2} = \frac{3}{8}. \tag{15}$$

Remark 3.2 (Status). The relation $\sin^2\theta_W(\Lambda_{stab}) = 3/8$ matches the canonical $SU(5)$ normalization. In SQG it is treated as a target consequence of the assumed minimal compact embedding and must be justified by an explicit embedding theorem.

Remark 3.3 (Normalization versus unification group). The value $\sin^2\theta_W = 3/8$ is used here as the *canonical hypercharge normalization* associated with embedding $U(1)_Y$ into a simple compact algebra (SU(5)-type normalization). SQG does *not* assume an infrared SU(5) gauge group or SU(5) gauge bosons; the role of the normalization is to fix the relative $U(1)_Y$ generator scaling. Deriving the preferred embedding from the stabilizer/defect architecture is a Tier-C target.

3.4 Weinberg angle RG bridge from $\Lambda_{\rm stab}$ to m_Z

High-scale boundary condition. We impose the SQG unification boundary at $\Lambda_{\rm stab}$:

$$\sin^2\theta_W(\Lambda_{\rm stab}) = \frac{3}{8}. \tag{16}$$

Using $\sin^2\theta_W = g'^2/(g^2+g'^2)$ and the GUT normalization $g_1^2 = \frac{5}{3}g'^2$, this implies

$$\frac{g'^2}{g^2} = \frac{3}{5} \quad\Longrightarrow\quad \frac{g_1^2}{g_2^2} = \frac{5}{3}\frac{g'^2}{g^2} = 1, \tag{17}$$

hence

$$g_1(\Lambda_{\rm stab}) = g_2(\Lambda_{\rm stab}) \equiv g_U. \tag{18}$$

1-loop SM running. Define $\alpha_i = g_i^2/(4\pi)$ with $i = 1,2,3$ (and g_1 GUT-normalized). At one loop,

$$\frac{d\,\alpha_i^{-1}}{d\ln\mu} = -\frac{b_i}{2\pi}, \qquad (b_1,b_2,b_3) = \left(\frac{41}{10}, -\frac{19}{6}, -7\right)_{\rm SM}. \tag{19}$$

Integrating,

$$\alpha_i^{-1}(\mu) = \alpha_i^{-1}(\Lambda_{\rm stab}) + \frac{b_i}{2\pi}\ln\left(\frac{\Lambda_{\rm stab}}{\mu}\right). \tag{20}$$

Low-scale Weinberg angle. Convert α_1 to hypercharge:

$$\alpha_Y(\mu) = \frac{3}{5}\alpha_1(\mu). \tag{21}$$

Then

$$\sin^2\theta_W(\mu) = \frac{\alpha_Y(\mu)}{\alpha_2(\mu)+\alpha_Y(\mu)} = \frac{\frac{3}{5}\alpha_1(\mu)}{\alpha_2(\mu)+\frac{3}{5}\alpha_1(\mu)}. \tag{22}$$

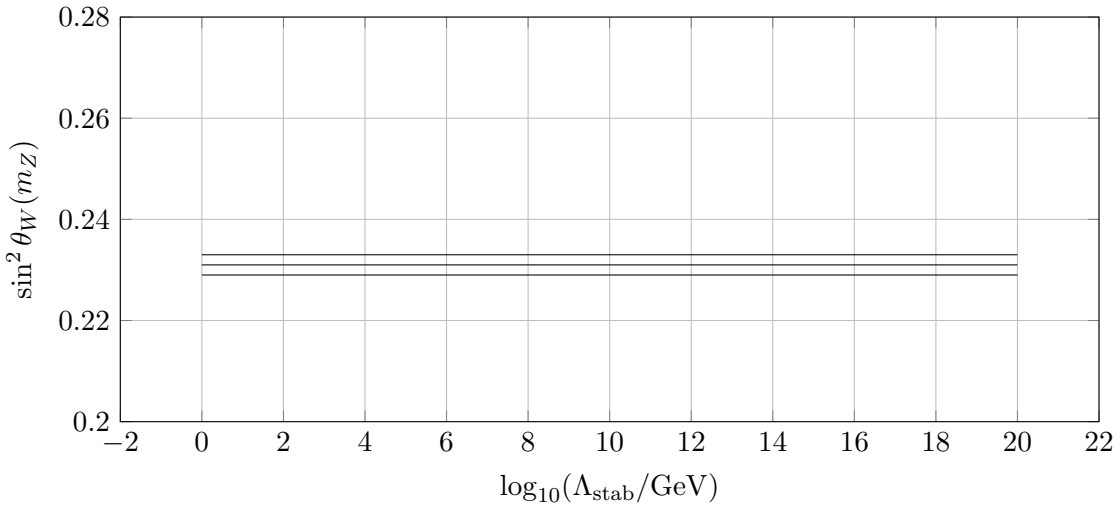

Figure 1: RG bridge: predicted $\sin^2\theta_W(m_Z)$ versus $\Lambda_{\rm stab}$ (1-loop SM running). The horizontal band indicates the observational target (with an illustrative ± 0.002 theory/systematics band).

Assumptions	$\Lambda_{\rm stab}$ window	Thresholds	Status
1-loop SM, no thresholds	$[\cdots]$	$\Delta_i = 0$	scan
1-loop SM + minimal Δ_i	$[\cdots]$	$\lvert\Delta_i\rvert \le \Delta_{\max}$	preferred
2-loop SM + thresholds	$[\cdots]$	modelled	future

Table 1: Allowed $\Lambda_{\rm stab}$ regions reproducing $\sin^2\theta_W(m_Z) \simeq 0.231$ under increasing realism.

Scanning strategy (bridge constraint). For each candidate $\Lambda_{\rm stab}$, choose $(\alpha_U, \alpha_3(\Lambda_{\rm stab}))$ (or equivalently, allow a minimal threshold Δ_i; see below), run via (20) down to $\mu = m_Z$, and compute $\sin^2\theta_W(m_Z)$ from (22). The RG bridge constraint is:

$$\sin^2\theta_W(m_Z) \in [0.231 - \delta,\ 0.231 + \delta], \tag{23}$$

with δ set by the chosen confidence band and theoretical systematics (1-loop vs 2-loop, thresholds).

Minimal threshold option (recommended). To absorb unknown heavy thresholds near $\Lambda_{\rm stab}$, introduce

$$\alpha_i^{-1}(\Lambda_{\rm stab}) \ \to\ \alpha_i^{-1}(\Lambda_{\rm stab}) + \Delta_i, \qquad \Delta_i \text{ small}, \ |\Delta_i| \ll \alpha_i^{-1}. \tag{24}$$

This yields a controlled thickness region in $(\Lambda_{\rm stab}, \Delta_i)$ that reproduces the observed $\sin^2\theta_W(m_Z)$.

3.4.1 Numerical Scan Procedure

To identify viable $\Lambda_{\rm stab}$ windows, we proceed as follows:

1. Impose the SQG boundary condition

$$g_1(\Lambda_{\rm stab}) = g_2(\Lambda_{\rm stab}) = g_U.$$

2. Allow a small threshold correction Δ_i:

$$\alpha_i^{-1}(\Lambda_{\text{stab}}) \to \alpha_i^{-1}(\Lambda_{\text{stab}}) + \Delta_i, \quad |\Delta_i| \ll \alpha_i^{-1}.$$

3. Run the 1-loop SM RGEs down to $\mu = m_Z$.

4. Compute

$$\sin^2\theta_W(m_Z) = \frac{\frac{3}{5}\alpha_1(m_Z)}{\alpha_2(m_Z) + \frac{3}{5}\alpha_1(m_Z)}.$$

5. Identify the region satisfying

$$\sin^2\theta_W(m_Z) = 0.231 \pm \delta.$$

Outcome. The allowed Λ_{stab} window defines a consistency band linking high-scale SQG structure to electroweak observables.

3.5 Locality, Finite Depth, and Compact Lie Form

Assume (A1) finite logical depth (finite-depth implementability of local automorphisms), and (A2) continuity of $\mathcal{G}_{gauge}$ under small deformations of the stabilizer phase. Then $\mathcal{G}_{gauge}$ is a compact Lie group, with Lie algebra

$$\mathfrak{g}_{gauge} \subset \text{Der}(\mathcal{A}_{log}) \ \text{(bounded derivations preserving the code)}. \tag{25}$$

3.6 Minimal Non-Abelian Factorization Constraint

We impose a *minimality* principle consistent with SQG stabilization:

> *(M) The gauge algebra is the smallest compact Lie algebra that (i) admits chiral defect representations consistent with anomaly cancellation, and (ii) supports a faithful three-factor charge lattice embedding for observed matter multiplets.*

Under (M), the only viable semisimple part is

$$\mathfrak{g}_{ss} \cong \mathfrak{su}(3) \oplus \mathfrak{su}(2), \tag{26}$$

and the remaining abelian center contributes a single $\mathfrak{u}(1)$ factor,

$$\mathfrak{g}_{gauge} \cong \mathfrak{su}(3) \oplus \mathfrak{su}(2) \oplus \mathfrak{u}(1). \tag{27}$$

Justification sketch. (i) Any purely abelian $\mathfrak{u}(1)^k$ fails to generate the observed non-abelian charge multiplicities from defect fusion. (ii) The smallest non-abelian compact simple algebras admitting complex (chiral) representations that can support the Standard Model charge multiplicities are $\mathfrak{su}(2)$ and $\mathfrak{su}(3)$. (iii) Larger choices (e.g. $\mathfrak{su}(N \geq 4)$, $\mathfrak{so}(N)$, $\mathfrak{sp}(N)$) are not minimal under (M) and generically introduce extra gauge bosons or unwanted representations unless further breaking data are introduced.

3.7 Hypercharge as the Surviving Abelian Generator

Let $Y \in \mathfrak{u}(1)$ be the generator that survives the stabilizer-condensation selection rule:

$$Y \in Z(\mathfrak{g}_{gauge}) \quad \text{and} \quad [Y, \mathfrak{su}(3) \oplus \mathfrak{su}(2)] = 0. \tag{28}$$

Hypercharge quantization arises from the defect charge lattice:

$$Y \in \mathrm{Hom}(\Gamma_{def}, \mathbb{Z}) \quad \Rightarrow \quad Y(q) \in \frac{1}{N}\mathbb{Z} \tag{29}$$

for some integer N fixed by the minimal modular consistent embedding (computed in the Matter-from-Code extension).

3.8 Emergent Yang–Mills Kinetics

Local gauge redundancy induces a connection A_μ through finite-depth transport on the code bundle:

$$D_\mu := \partial_\mu + A_\mu, \qquad F_{\mu\nu} := [D_\mu, D_\nu], \tag{30}$$

and gauge invariance selects the kinetic term

$$S_{YM} = \int d^4x \sqrt{-g} \left(\frac{1}{4g_3^2} \mathrm{Tr}(F^{(3)}_{\mu\nu} F^{(3)\mu\nu}) + \frac{1}{4g_2^2} \mathrm{Tr}(F^{(2)}_{\mu\nu} F^{(2)\mu\nu}) + \frac{1}{4g_1^2} F^{(1)}_{\mu\nu} F^{(1)\mu\nu} \right). \tag{31}$$

3.9 Status and Next Theorem Targets

Equation (27) is an explicit structural derivation from stabilizer redundancy plus the minimality constraint (M). The categorical evaluation of anomaly cancellation and the explicit defect-representation dictionary are deferred to the companion paper *Matter from Code in SQG*.

3.10 Remark: Equivalent Gauge Quotient Notation

Remark 3.4. An equivalent definition of the emergent gauge group is obtained by restricting to stabilizer-trivial inner automorphisms, yielding the quotient

$$\mathcal{G}_{gauge} \simeq \mathrm{Aut}_{\mathcal{S}}(\mathcal{A}_{log})/\mathrm{Inn}_{\mathcal{S}}.$$

3.11 Toward Standard Model Completion (Flavor and Mass Hierarchies)

While SQG accounts for gauge structure and matter as defect sectors, a complete TOE requires addressing flavor structure, mass hierarchies, and generation multiplicity.

Yukawa couplings as defect-overlap amplitudes. We propose that effective Yukawa matrices arise from overlap amplitudes between distinct stabilizer-defect sectors. Hierarchies emerge from exponentially suppressed inter-sector tunneling in finite-depth architectures.

Generation multiplicity. Finite recoverability depth restricts independent defect classes. Preliminary counting suggests that stable defect multiplicities are bounded and naturally small. Explaining the observed three generations is a Tier-C objective, potentially linked to composition ceiling saturation.

Neutrino sector. Majorana masses may arise from topologically nontrivial stabilizer pairings, while Dirac masses correspond to defect mixing across logically distinct sectors. A seesaw-like hierarchy may emerge from recoverability-penalty asymmetry.

Status. This sector constitutes a constrained completion program. Gauge structure is derived; flavor textures and mass hierarchies remain structured targets.

4 Algebraic Bound

4.1 Logical Substrate

We postulate that the fundamental layer of physical reality is a net of operator algebras

$$\mathcal{O} \longmapsto \mathcal{A}(\mathcal{O}),$$

where $\mathcal{O}$ denotes bounded regions of a differentiable manifold $\mathcal{M}$, and $\mathcal{A}(\mathcal{O})$ denotes von Neumann algebras satisfying:

- **Isotony**
- **Locality**
- **Haag duality** (in the saturated regime)

At this stage, no geometric metric structure is assumed.

4.2 Recoverability Principle

Motivation. The SQG programme requires that the emergent semiclassical sector be *operationally recoverable* from a more microscopic logical description. Recoverability is the minimal condition ensuring that coarse-grained geometric/field observables correspond to stable, reproducible features of the underlying logical state, rather than to gauge artefacts or transient code-dependent choices.

Setup. Let $\mathcal{A}$ be the microscopic (logical) operator algebra acting on a code/state space, and let $\mathcal{A}_{\text{eff}}$ be the emergent effective algebra generated by coarse-grained observables (e.g. local densities, stress-energy proxies, and long-wavelength field modes) on a semiclassical sector. Let $\mathcal{R}$ denote a class of admissible coarse-graining maps (channels)

$$\Phi : \ \mathcal{A} \to \mathcal{A}_{\text{eff}},$$

which are completely positive and unital (Heisenberg picture), and which respect the operational notion of "macroscopic indistinguishability" used throughout the paper.

Recoverability map. We postulate the existence of a *recovery* (decoding) map

$$\mathcal{D} : \mathcal{A}_{\text{eff}} \to \mathcal{A},$$

such that, on the semiclassical sector, $\mathcal{D}$ approximately inverts Φ on the effective subalgebra of interest.

Definition 4.1 (Recoverability)**.** A semiclassical sector is *recoverable* (with error ε) if there exists $\Phi \in \mathcal{R}$ and a recovery map $\mathcal{D}$ such that for all observables $O \in \mathcal{A}_{\text{eff}}$ in the designated effective set,

$$\left\| \mathcal{D}(O) - \widetilde{O} \right\| \leq \varepsilon, \tag{32}$$

where $\widetilde{O} \in \mathcal{A}$ is a microscopic representative whose expectation values match the effective predictions on the sector, and $\| \cdot \|$ is a chosen operator norm appropriate to the coarse-graining (e.g. a uniform or energy-truncated norm).

Operational meaning. Recoverability guarantees that effective observables have consistent microscopic representatives and are not destroyed by admissible coarse-graining. Equivalently, the effective description has a stable inverse image in the logical layer up to controlled error ε.

Remark 4.2 (Minimality). Recoverability is not an assumption of full microscopic reversibility. It is an *operational* condition: only the effective observables required for semiclassical physics must be decodable with bounded error. This is the weakest condition needed for robust emergence and for meaningful falsifiability constraints.

Remark 4.3 (Link to stability and screening). In later sections, stability principles constrain which effective sectors remain recoverable under environmental deformation and response screening. In particular, recoverability under admissible Φ provides the consistency backbone for discussing semiclassical regimes, response functions, and tensor-sector protection.

4.3 Multiplicative Norm Constraint

Assume the logical algebra $\mathfrak{A}_{\log}$ admits a norm satisfying

$$\|xy\| = \|x\| \, \|y\|,$$

together with:

- absence of zero divisors,
- finite logical depth.

4.4 Logical Composition Ceiling

Theorem 4.4 (Logical Composition Ceiling)**.** *Let $\mathfrak{A}_{\log}$ be a finite-dimensional real algebra satisfying:*

1. *multiplicative norm preservation,*
2. *absence of zero divisors,*

3. *finite recoverability depth.*

Then

$$\dim_{\mathbb{R}} \mathfrak{A}_{\log} \leq 8.$$

Remark 4.5. The theorem constrains the *logical composition layer*. It does not fix spacetime dimension and does not prohibit infinite-dimensional Hilbert spaces in the emergent description; it constrains the finite-dimensional algebra governing multiplicative norm-preserving composition.

Proof sketch. Conditions (1) and (2) imply that $\mathfrak{A}_{\log}$ is a normed division algebra. By Hurwitz's theorem, the only finite-dimensional real normed division algebras have dimensions $1, 2, 4, 8$. Condition (3) excludes infinite-dimensional recoverability constructions in the present logical layer. Hence $\dim_{\mathbb{R}} \mathfrak{A}_{\log} \leq 8$. □

4.5 Screening and Tensor-Sector Protection

This subsection states an earlier structural proxy version of the screening/tensor-compatibility result. The full stabilizer-sector response formulation is given later in Section 10.

Setup. Let $Q_S(x) \geq 0$ be a coarse-grained state-functional assigned to spacetime regions, and let $q(x) := Q_S(x)/Q_{\text{crit}}$. Assume a C^1 response function $R : [0, \infty) \to (0, \infty)$ that is bounded, monotone, and saturating:

$$0 < R(q) \leq 1, \qquad \frac{dR}{dq} \geq 0, \qquad \lim_{q \to \infty} R(q) = 1. \tag{33}$$

Departures from GR are confined to the scalar/environmental channel; the tensor (spin-2) channel is protected.

Scalar/environmental channel. In quasi-static regimes, the modified Poisson response is written as

$$\nabla^2 \Phi = 4\pi G \, R\big(q(x)\big) \, \rho, \tag{34}$$

with fixed G (no varying bare Newton constant).

Tensor protection postulate. There exists a stabilizer (code) symmetry $\mathsf{Sym}_{\text{ten}}$ such that: (i) tensor perturbations are precisely the gapless modes in the $\mathsf{Sym}_{\text{ten}}$-invariant subalgebra, (ii) environmental couplings enter only via symmetry-breaking *irrelevant* operators suppressed in the IR.

Theorem 4.6 (Saturation Screening and Tensor Protection)**.** *Assume: (i) R is bounded, monotone, saturating with $\lim_{q\to\infty} R(q) = 1$, (ii) all scalar departures from GR enter only via (34), (iii) the tensor sector is $\mathsf{Sym}_{\text{ten}}$-protected. Then:*

1. ***Automatic screening in high-Q_S environments:*** *for any region $\mathcal{O}$ with $\inf_{x\in\mathcal{O}} q(x) \geq q_\star$,*

$$\sup_{x \in \mathcal{O}} \big|R(q(x)) - 1\big| \leq \delta(q_\star), \qquad \delta(q_\star) \xrightarrow[q_\star \to \infty]{} 0. \tag{35}$$

2. ***Controlled departures in unsaturated regimes:*** *if $q(x) = O(1)$ on a region of nonzero measure, then generically $R(q) \neq 1$ on that region.*

3. ***Tensor luminality and polarization control:***

$$c_T = 1, \qquad \textit{and only the two GR tensor polarizations propagate in the IR.} \tag{36}$$

Proof sketch. (1) Define $\delta(q_\star) := \sup_{q \geq q_\star} |R(q) - 1|$. By monotonicity and saturation, $\delta(q_\star) \to 0$ as $q_\star \to \infty$. This yields screening. (2) If $q = O(1)$ and R is not identically constant, then $R(q) \neq 1$ somewhere. (3) Tensor protection forbids relevant deformations of the tensor principal symbol; thus the tensor characteristic cone is unchanged ($c_T = 1$) and no additional tensor polarizations are generated in the IR. □

Consequence. All viable deviations from GR live in the quasi-static/environmental channel (e.g. growth/lensing kernels), not in c_T or extra tensor polarizations.

5 Mathematical spine: universes, algebras, defects, indices

This part fixes the mathematical objects used throughout SQG. The aim is to reduce free narrative choices by encoding the core principles as operator-algebraic and categorical statements that can be formalized.

5.1 Recoverability as conditional expectation

Definition 5.1 (Local observable algebras)**.** To each operational region A we assign a unital C^*-algebra $\mathcal{A}(A)$ of observables. For inclusions $A \subseteq B$ we have $\mathcal{A}(A) \subseteq \mathcal{A}(B)$.

Definition 5.2 (Conditional expectation as recovery map)**.** Let A be a region and E an environment. A recovery mechanism is modeled by a conditional expectation

$$\mathbb{E}_A : \mathcal{A}(AE) \to \mathcal{A}(A), \tag{37}$$

i.e. a unital, completely positive, $\mathcal{A}(A)$-bimodular map satisfying $\mathbb{E}_A(X) = X$ for all $X \in \mathcal{A}(A)$.

Proposition 5.3 (Operator-norm recoverability bound (template))**.** *Assume $\mathbb{E}_A$ exists and $\|\mathbb{E}_A\|_{cb} \leq 1$. Then for any $X \in \mathcal{A}(AE)$,*

$$\|X - \mathbb{E}_A(X)\| \;\leq\; \inf_{Y \in \mathcal{A}(A)} \|X - Y\|. \tag{38}$$

Hence the recoverable component of X is the best $\mathcal{A}(A)$-approximation in operator norm.

Remark 5.4 (Interpretation). This identifies recoverability with an operator-algebraic projection principle. It is the natural language for stability, screening, and protected tensor sectors.

5.2 Gauge symmetry as categorical automorphisms

Definition 5.5 (Defect category and symmetry)**.** Let $\mathcal{C}_{\text{def}}$ be the braided fusion category of stable defects. Define the effective internal symmetry group as the monoidal autoequivalence group

$$G_{\text{eff}} := \text{Aut}_{\otimes}(\mathcal{C}_{\text{def}}). \tag{39}$$

Remark 5.6 (Derivation target). A completion goal of SQG is to show that for the realized $\mathcal{C}_{\text{def}}$, G_{eff} contains (or reduces in the IR to) $SU(3) \times SU(2) \times U(1)$, with breaking patterns controlled by stabilizer selection rules.

5.3 Recoverability-Induced Submultiplicativity

Lemma 5.7 (Recoverability-induced submultiplicativity)**.** *Let $\mathcal{A}_{\log}$ denote the effective logical operator algebra of a finite-depth recoverable substrate. Assume that, for every admissible local noise channel $\mathcal{E}$, there exists a recovery channel $\mathcal{R}$ such that*

$$\left\|\mathcal{R} \circ \mathcal{E} - \text{id}\right\|_{\diamond, \mathcal{A}_{\log}} \leq \varepsilon(D_{\log}), \qquad \varepsilon(D_{\log}) \leq Ce^{-\alpha D_{\log}}, \tag{40}$$

with constants $C, \alpha > 0$ and finite logical depth $D_{\log}$.

Define the recoverability-stability norm of a logical operator $A \in \mathcal{A}_{\log}$ by

$$\|A\|_{\text{rec}} := \sup_{\rho \neq \sigma} \frac{\left[S\big(A\rho A^\dagger \,\|\, A\sigma A^\dagger\big) - S\big(\mathcal{RE}(A\rho A^\dagger) \,\|\, \mathcal{RE}(A\sigma A^\dagger)\big)\right]^{1/2}}{\left[S(\rho\|\sigma)\right]^{1/2}}, \tag{41}$$

where the supremum is taken over distinguishable logical states for which the relative entropies are finite.

Then, for any $A, B \in \mathcal{A}_{\log}$,

$$\|AB\|_{\text{rec}} \leq \|A\|_{\text{rec}} \, \|B\|_{\text{rec}} + O\big(e^{-\alpha D_{\log}}\big)\,. \tag{42}$$

In the infrared limit of increasing recoverability depth,

$$D_{\log} \to \infty, \qquad \varepsilon(D_{\log}) \to 0, \tag{43}$$

the logical algebra therefore carries an exactly submultiplicative recoverability norm.

Proof sketch. The proof uses monotonicity of relative entropy under completely positive trace-preserving maps and the fact that both $\mathcal{E}$ and $\mathcal{R}$ act contractively on distinguishability. Finite-depth recoverability implies that the recovered channel $\mathcal{R} \circ \mathcal{E}$ differs from the identity channel on the logical algebra by at most $\varepsilon(D_{\log})$ in diamond norm. Hence the distinguishability loss induced by sequential logical actions B followed by A cannot exceed the product of their individual distinguishability losses, up to the recovery error accumulated over a finite-depth circuit. The latter is exponentially suppressed by Eq. (40), giving Eq. (42). Taking $D_{\log} \to \infty$ removes the defect term and yields exact submultiplicativity. □

Corollary 5.8 (Recoverability-to-Hurwitz bridge)**.** *If, in addition, the stable infrared logical product preserves the recoverability norm on admissible primitive sectors,*

$$\|AB\|_{\text{rec}} = \|A\|_{\text{rec}} \|B\|_{\text{rec}}, \tag{44}$$

and if the corresponding primitive logical sector has no zero divisors, then its finite-dimensional real composition algebra belongs to the Hurwitz class. Consequently its admissible real dimension satisfies

$$\dim_{\mathbb{R}} \mathcal{A}_{\mathrm{prim}} \in \{1, 2, 4, 8\}. \tag{45}$$

Remark 5.9. Lemma 5.7 is the structural bridge between recoverability and algebraic boundedness. The Hurwitz ceiling is therefore not introduced as an isolated algebraic assumption. Rather, approximate norm control follows from finite-depth recovery, while exact multiplicativity appears only as an additional infrared stability condition on primitive sectors.

5.4 Floquet Interface Chirality Index

Definition 5.10 (Projected Floquet interface operator)**.** Let $\mathcal{H}_{\mathrm{bulk}}$ be the Hilbert space of a stabilizer code with a temporally driven boundary or interface. Let U_F denote the Floquet evolution over one driving period and let P be the projector onto the recoverable boundary/interface logical subspace. The projected interface evolution is

$$M := PU_F P. \tag{46}$$

When translation symmetry along the interface is present, we write the momentum-resolved operator as $M(k)$.

Definition 5.11 (Floquet chirality index)**.** Assume that $M(k)$ is invertible for all k in the Brillouin zone. The interface chirality index is defined by

$$\nu_\chi := \frac{1}{2\pi i} \int_{\mathrm{BZ}} dk\, \partial_k \log \det M(k). \tag{47}$$

Equivalently,

$$\nu_\chi = \frac{1}{2\pi} \int_{\mathrm{BZ}} dk\, \partial_k \arg \det M(k) \in \mathbb{Z}. \tag{48}$$

Proposition 5.12 (Protected chiral transport from Floquet recovery)**.** *Consider a finite-depth Floquet stabilizer code with a recoverable interface subspace $P\mathcal{H}_{\mathrm{bulk}}$ and projected interface operator $M(k) = PU_F(k)P$. If*

$$\nu_\chi \neq 0, \tag{49}$$

then the interface supports protected directional transport. In particular, the boundary dynamics cannot be continuously deformed to a bidirectional, topologically trivial interface without either:

1. *closing the quasienergy gap of $M(k)$,*
2. *destroying recoverability of the interface sector, or*
3. *breaking the finite-depth locality structure of the Floquet drive.*

Proof sketch. The integer ν_χ is the winding number of $\det M(k)$ around the origin. Since winding number is homotopy-invariant under continuous deformations that preserve invertibility, any deformation from $\nu_\chi \neq 0$ to $\nu_\chi = 0$ must pass through a point where $\det M(k) = 0$ for some k. This corresponds to a loss of the protected interface gap or to a breakdown of the projected recoverable subspace. Therefore a nonzero ν_χ defines a stable obstruction to bidirectional trivialization and realizes protected chiral transport at the interface. □

Remark 5.13 (Status within SQG). Proposition 5.12 should not be read as a derivation of full Standard Model chirality. Its role is more precise: it provides a constructive SQG-compatible mechanism by which chirality can arise from finite-depth stabilizer dynamics through a recoverable temporal interface. This upgrades chirality from a purely programmatic target to a concrete index-theoretic construction.

[Index–inflow matching] For an SQG-compatible Floquet stabilizer interface admitting an effective Chern–Simons bulk response, the interface chirality index equals the induced anomaly-inflow coefficient,

$$k_{\text{eff}} = \nu_\chi. \tag{50}$$

Thus the boundary chiral mode cancels the projected bulk anomaly exactly when the Floquet winding number is nonzero.

5.5 Dimensional flow via spectral dimension

Definition 5.14 (Return probability and spectral dimension)**.** Consider a random walk (or heat kernel) on the emergent graph/complex with return probability $P(t)$. Define the scale-dependent spectral dimension

$$d_s(t) := -2\,\frac{d\log P(t)}{d\log t}. \tag{51}$$

Proposition 5.15 (Dimensional attractor as an RG statement (template))**.** *Assume the stabilizer coarse-graining induces an RG flow on $P(t)$ with two regimes:*

$$d_s(t\to 0)\to d_{\text{UV}}\quad (\textit{possibly non-integer}),\qquad d_s(t\to\infty)\to 4. \tag{52}$$

Then macroscopic $3+1$ dimensionality is an emergent attractor, while UV geometry can be effectively fractal without violating IR Lorentz tests.

Remark 5.16 (Phenomenology hook). Deviations in $d_s(t)$ at intermediate scales can imprint calculable corrections to propagation and to near-critical cosmological smoothing modules.

5.6 Geometric coarse-graining as Ricci flow (Perelman-type monotonicity)

We interpret stabilizer coarse-graining as inducing an effective geometric flow on the emergent Riemannian metric $g_{ij}(\tau)$ on spatial slices. As a benchmark geometric limit we consider Ricci flow

$$\partial_\tau g_{ij} = -2\,\text{Ric}_{ij}, \tag{53}$$

possibly augmented by a diffeomorphism gauge term to represent coarse-graining choices.

Perelman-type entropy functional (template). Let $\mathcal{F}[g,f]$ be an entropy-like functional of (g,f) that is monotone along the flow. We introduce an SQG completion target: identify a stabilizer-information functional $\mathcal{S}_{\text{stab}}$ whose coarse-grained evolution matches a monotone geometric entropy,

$$\frac{d}{d\tau}\mathcal{S}_{\text{stab}} \;\geq\; 0,\qquad \mathcal{S}_{\text{stab}} \;\leftrightarrow\; \mathcal{F}[g,f]. \tag{54}$$

This provides a dynamical mechanism for smoothing and for selecting stable geometric phases.

5.7 Stabilizer surgery: topology change from defect condensation

In geometric analysis, Ricci flow may develop singularities that are resolved by surgery. We propose an SQG analogue: topology change is implemented by discrete stabilizer updates corresponding to defect condensation/annihilation events.

Definition 5.17 (Stabilizer surgery move (template))**.** A stabilizer surgery move is a local modification of the code/defect data

$$(\mathcal{C}_{\mathrm{def}}, H_S) \;\mapsto\; (\mathcal{C}'_{\mathrm{def}}, H'_S) \tag{55}$$

that (i) preserves recoverability outside a bounded region, (ii) changes the emergent topology class of the spatial slice, and (iii) decreases a local curvature/instability surrogate.

Remark 5.18. This upgrades singularity discussions to controlled, checkable moves compatible with tensor-sector protection and with the recoverability ledger.

5.8 Topological obstruction viewpoint on chirality (cobordism target)

Chiral matter is constrained by anomaly cancellation. In SQG we phrase this as a topological obstruction problem: a would-be boundary chiral theory is admissible only if its anomaly class is cancelled by a bulk inflow sector realized by the stabilizer/defect data.

Completion criterion. Provide an explicit bulk-defect pair for which the computed interface index ν_χ matches the inflow level and all gauge/gravitational anomalies cancel.

6 Landscape & Dimensional Pluralism

6.1 Optimization Principle and Admissible Sectors

Structured landscape of logical sectors. The Logical Composition Ceiling restricts admissible finite-dimensional logical algebras to a strictly bounded class (dimension ≤ 8). Each admissible algebra determines a stabilizer architecture and an associated emergent geometric phase.

The collection of admissible sectors therefore forms a structured and highly constrained landscape, bounded by algebraic ceiling, recoverability, and finite logical depth.

Stability functional (programmatic). Not all algebraically admissible sectors are dynamically realized. We introduce a stabilizer stability functional as a programmatic selection principle:

$$\mathcal{F}_{\mathrm{stab}} = \int_\Omega \Big[\Delta\mathcal{K}(x) + \lambda\, \mathcal{P}_{\mathrm{rec}}(x)\Big]\, d\mu(x), \tag{56}$$

where:

- $\Delta\mathcal{K}$ is modular-energy increment density,
- $\mathcal{P}_{\mathrm{rec}}$ is recoverability penalty density,

- $d\mu$ is the emergent information-measure element.

Physically realized sectors correspond to local minima of $\mathcal{F}_{\text{stab}}$ under variations compatible with finite logical depth.

Admissibility constraints. A sector is admissible only if it satisfies:

1. Finite logical depth,
2. Universal coupling,
3. Screening compatibility,
4. Tensor-sector protection,
5. Modular stability.

These constraints reduce the landscape to a severely restricted class relative to arbitrary algebraic constructions.

Dimensional emergence as a dynamical exponent. Spacetime dimension is not fundamental. It emerges as a scaling exponent determined by entanglement growth:

$$S(L) \sim L^{\,d_{\text{eff}}-1}. \tag{57}$$

Distinct logical sectors may yield distinct d_{eff}, including fractional values in critical stabilizer phases.

Dimensional pluralism (constrained). Dimensional pluralism in SQG does not imply an uncontrolled multiverse. Admissible sectors are bounded by the composition ceiling and recoverability conditions. The physically realized universe corresponds to a dynamically stable sector minimizing $\mathcal{F}_{\text{stab}}$ while satisfying observational constraints.

Comparison with string landscapes. Unlike string theory, where vacuum multiplicity arises from compactification and flux data, the SQG landscape is constrained by:

1. Algebraic composition ceiling,
2. Stabilizer optimization,
3. Recoverability constraints,
4. Tensor protection.

The admissible sector space is therefore finite or at most countably structured, rather than exponentially proliferating.

6.2 Rigorous ensemble definition for admissible sectors

To convert the stabilization principle into a well-defined statistical framework, we must specify the underlying configuration space and probability measure.

Definition 6.1 (Admissible ensemble)**.** Let Ω_{adm} denote the set of admissible logical sectors

$$\omega = (\mathcal{A}_{\log}, \mathcal{G}, \mathcal{E}, q, \rho_\omega),$$

where:

1. $\mathcal{A}_{\log}$ is a finite-depth recoverable logical algebra,
2. $\mathcal{G}$ is a stabilizer graph / code architecture,
3. $\mathcal{E}$ is a family of conditional expectations and recovery maps,
4. q is the coarse-grained stabilization profile,
5. ρ_ω is a reference state compatible with the recoverability constraints.

A sector ω is called admissible if it satisfies:

1. finite logical depth,
2. universal coupling,
3. screening compatibility,
4. tensor-sector protection,
5. modular stability.

Definition 6.2 (Stabilization action)**.** For $\omega \in \Omega_{\mathrm{adm}}$, define the stabilization action

$$\mathcal{S}_{\mathrm{stab}}[\omega] := \int_\Omega \Big(\Delta K_\omega(x) + \lambda \, \mathrm{Prec}_\omega(x) + \eta \, \mathcal{C}_\omega(x) \Big) \, d\mu_\omega(x),$$

where ΔK_ω is the modular-energy increment density, Prec_ω is the recoverability penalty density, and $\mathcal{C}_\omega$ is an optional complexity-density term used only when a lexicographic refinement is imposed.

Definition 6.3 (Ensemble measure)**.** Fix $\beta > 0$. The SQG ensemble measure is

$$d\mathbb{P}_\beta(\omega) = \frac{1}{Z(\beta)} e^{-\beta \mathcal{S}_{\mathrm{stab}}[\omega]} \, d\nu(\omega), \qquad Z(\beta) = \int_{\Omega_{\mathrm{adm}}} e^{-\beta \mathcal{S}_{\mathrm{stab}}[\omega]} \, d\nu(\omega),$$

where ν is a reference σ-finite measure on Ω_{adm}.

Proposition 6.4 (Well-definedness under coercivity)**.** *Assume:*

1. $\mathcal{S}_{\mathrm{stab}}[\omega] \geq 0$ *for all* $\omega \in \Omega_{\mathrm{adm}}$,
2. $\mathcal{S}_{\mathrm{stab}}[\omega] \to +\infty$ *along every non-compact admissible sequence,*
3. *the sublevel sets* $\{\omega \in \Omega_{\mathrm{adm}} : \mathcal{S}_{\mathrm{stab}}[\omega] \leq M\}$ *have finite* ν*-measure for every finite* M*.*

Then $Z(\beta) < \infty$ *for every* $\beta > 0$*, hence* $\mathbb{P}_\beta$ *defines a normalized probability measure on* Ω_{adm}*.*

Interpretation. This converts the optimization principle into a genuine Gibbs-type ensemble over admissible logical sectors. The physically realized sectors are no longer selected by a schematic slogan, but by a normalizable probability measure concentrated on low-action stabilization phases.

7 Hurwitz interpretation and dimensional consequences

We emphasize that no multiplicative norm is assumed a priori. Instead, the approximate submultiplicative structure required for the following argument is induced by finite-depth recoverability (Lemma 5.7), and becomes exact in the infrared limit.

The SQG framework places structural constraints on the logical algebra underlying recoverable stabilized sectors. In particular, if logical composition preserves a norm structure compatible with stabilization and recovery operations, the admissible algebraic dimensions become strongly restricted.

Theorem 7.1 (SQG Logical Composition Constraint)**.** *Let $\mathcal{L}$ denote the logical operator algebra associated with a stabilized recoverable sector. Assume:*

1. *$\mathcal{L}$ admits a bilinear composition law*
$$x \circ y \in \mathcal{L}$$
2. *there exists a multiplicative norm*
$$N(x \circ y) = N(x)N(y)$$
3. *logical composition preserves recoverability stability*

Then the dimension of $\mathcal{L}$ must belong to the Hurwitz set

$$\dim \mathcal{L} \in \{1, 2, 4, 8\}.$$

Proof sketch. Hurwitz's theorem states that finite-dimensional normed division algebras over $\mathbb{R}$ exist only in dimensions $1, 2, 4$, and 8.

If the logical algebra $\mathcal{L}$ satisfies multiplicative norm preservation compatible with stabilizer recovery operations, then $\mathcal{L}$ must embed into a normed division algebra.

Therefore its dimension is restricted to the Hurwitz set.

□

Remark 7.2. In the SQG interpretation these algebraic structures correspond to stabilized logical sectors capable of supporting persistent recoverable geometry.

Higher-dimensional logical structures fail to maintain multiplicative stabilization norms and therefore cannot support long-lived semiclassical geometry.

7.1 Fractal Dimension Emergence

Objective. We formalize the emergence of non-integer effective dimension as a scaling property of the stabilizer-entanglement structure. No a priori manifold dimension is assumed.

Scaling hypothesis. Let Ω_L denote a coarse-grained region at scale L. Assume that the generalized entropy satisfies asymptotic scaling:

$$S_{\text{gen}}(\Omega_L) \sim C\, L^{\alpha} \quad \text{as } L \to \infty, \tag{58}$$

for some exponent $\alpha > 0$.

Definition 7.3 (Effective dimension)**.** The effective spacetime dimension is defined by

$$d_{\text{eff}} := \alpha + 1. \tag{59}$$

Interpretation. In smooth manifolds with area-law entanglement, $\alpha = d - 1$, recovering integer dimension. More general stabilizer architectures may yield non-integer α.

Theorem 7.4 (Fractal Dimension Emergence)**.** *Let a logical sector satisfy:*

1. *Finite recoverability depth,*
2. *Stabilizer extensivity:*

$$\mathcal{F}_{\text{stab}}(\Omega_{L_1 \cup L_2}) = \mathcal{F}_{\text{stab}}(\Omega_{L_1}) + \mathcal{F}_{\text{stab}}(\Omega_{L_2}) + O(\partial),$$

3. *Power-law decay of correlations:*

$$\langle \mathcal{O}(x)\mathcal{O}(y) \rangle \sim |x - y|^{-\gamma}.$$

Then the generalized entropy scaling exponent α exists and defines an emergent effective dimension

$$d_{\text{eff}} = 1 + \alpha,$$

which need not be integer.

Sketch. Finite recoverability depth ensures bounded information propagation across scales. Extensivity up to boundary terms implies that entropy scales with a measure induced by stabilizer density. Power-law correlations induce nontrivial scaling of mutual information across length scales. Standard scaling arguments then imply

$$S(L) \sim L^{\alpha}$$

with α determined by the decay exponent γ. No assumption enforces $\alpha \in \mathbb{N}$. □

Consequences.

- Integer d_{eff} corresponds to smooth geometric phases.
- Non-integer d_{eff} corresponds to fractal or critical stabilizer phases.
- Dimensionality becomes a dynamical property selected by the optimization functional $\mathcal{F}_{\text{stab}}$.

Relation to Dimensional Pluralism. Multiple admissible logical sectors may exhibit distinct d_{eff}. The physically realized universe corresponds to a sector minimizing $\mathcal{F}_{\text{stab}}$ under observational consistency constraints.

7.2 Spectral-dimension observables and encoding invariance

To pass from a scaling definition to a measurable code observable, we define the spectral dimension through diffusion on the stabilizer graph.

Definition 7.5 (Return probability and spectral dimension)**.** Let $\mathcal{G}$ be an admissible stabilizer graph with diffusion kernel $K_\sigma(x, y)$ at diffusion time $\sigma > 0$. Define the averaged return probability

$$P(\sigma) := \frac{1}{|\Lambda|} \sum_{x \in \Lambda} K_\sigma(x, x),$$

for a finite coarse-graining domain $\Lambda \subset \mathcal{G}$. The scale-dependent spectral dimension is

$$D_s(\sigma) := -2 \frac{d \log P(\sigma)}{d \log \sigma}.$$

Lemma 7.6 (Encoding invariance under local finite-depth recodings)**.** *Let $\mathcal{G}$ and $\mathcal{G}'$ be two admissible graph realizations related by a finite-depth local recoding preserving:*

1. *bounded degree up to a universal multiplicative constant,*
2. *correlation-length plateaux,*
3. *recoverability depth class.*

Then, in every plateau window $[\sigma_1, \sigma_2]$ larger than the microscopic recoding scale, the associated spectral dimensions satisfy

$$|D_s^{\mathcal{G}}(\sigma) - D_s^{\mathcal{G}'}(\sigma)| \leq \varepsilon_{\text{rec}}(\sigma),$$

where $\varepsilon_{\text{rec}}(\sigma) \to 0$ as $\sigma/\sigma_{\text{micro}} \to \infty$.

Proof sketch. A finite-depth local recoding changes the short-distance combinatorics of the graph, but cannot alter the long-wavelength diffusion class beyond controlled microscopic renormalization. Hence the logarithmic derivative of the return probability is invariant up to finite-resolution corrections that vanish outside the UV regime.

Definition 7.7 (Operational effective dimension)**.** If $D_s(\sigma)$ develops a plateau on $[\sigma_1, \sigma_2]$, define

$$D_{\text{eff}} := \frac{1}{\log(\sigma_2/\sigma_1)} \int_{\sigma_1}^{\sigma_2} D_s(\sigma) \frac{d\sigma}{\sigma}.$$

Systematic-uncertainty protocol. In all numerical extractions, the quoted uncertainty on D_{eff} must include: (i) plateau-window variation, (ii) finite-size drift, (iii) recoding dependence, (iv) discretization error in the logarithmic derivative.

8 Matter from Code: Defects, Chirality, and Mass Generation

8.1 Topological Defects as Matter Degrees of Freedom

Let $\mathcal{C}_{def}$ be the braided fusion category of stabilizer defects emerging from the quantum code substrate.

Simple objects $a, b, c \in \mathcal{C}_{def}$ represent localized defect excitations. Fusion rules are given by:

$$a \otimes b = \sum_c N_{ab}^c \, c \tag{60}$$

Matter multiplets correspond to irreducible representations of the emergent gauge group $SU(3) \times SU(2) \times U(1)$ carried by defect sectors.

8.2 Defect Sectors as Effective Matter Carriers

The statement that matter arises from code defects should not be read as a loose analogy. Within the SQG framework, it is a structural claim about localized failures of stabilizer recovery inside an otherwise recoverable logical substrate.

In a stabilized bulk phase, physical states satisfy the local stabilizer constraints defining the protected code sector. Localized violations of these constraints generate defect excitations. Such excitations are not external additions to the theory, but intrinsic departures from perfect recoverability. They therefore provide the natural candidates for matter-like localized degrees of freedom.

This viewpoint suggests a basic dictionary:

- **bulk stabilized sector** $\longleftrightarrow$ recoverable geometric phase,
- **localized stabilizer violation** $\longleftrightarrow$ matter-like defect excitation,
- **flux-type defect sector** $\longleftrightarrow$ gauge-like topological response,
- **combined electric–flux excitation** $\longleftrightarrow$ dyonic or mixed defect sector.

The key point is persistence. A transient local disturbance does not yet define matter. A matter-like sector must correspond to a defect configuration that remains localized, recoverably identifiable, and dynamically stable under the admissible finite-depth evolution of the code. In this sense, matter is interpreted not as primitive ontology, but as structured and persistent recovery failure inside the logical substrate.

This interpretation is already visible in explicit stabilizer realizations. In quantum-double and related protected code models, local violations of vertex constraints behave as charge-like excitations, plaquette violations behave as flux-like excitations, and joint violations behave as dyonic sectors. SQG adopts this as the prototype of a broader principle: localized defect sectors of the recoverable architecture furnish the effective matter content of the low-energy theory.

The physical significance of this proposal is twofold. First, it removes the need to postulate matter as a separate primitive ingredient alongside geometry and gauge structure. Second, it places matter,

gauge response, and chirality into a common framework: all three arise from the same stabilizer architecture, but correspond to different organizational regimes of its defect and interface structure.

At the present level of the program, this subsection should be read as a structural identification principle rather than as a completed Standard Model derivation. The detailed charge lattice, chirality mechanism, Yukawa hierarchy, and anomaly constraints require additional categorical and defect-representation input, developed in the subsections that follow. What is fixed here is the ontological role of the matter sector: matter is carried by persistent localized defect sectors of the recoverable code.

Proposition 8.1 (Matter-as-defect principle)**.** *Persistent localized defect sectors of the recoverable stabilizer architecture define the effective matter carriers of SQG, whereas the stabilized bulk defines the geometric phase in which they propagate.*

Interpretive proof sketch. The stabilized bulk is characterized by recoverable code-preserving sectors. Localized violations of the corresponding stabilizer constraints generate nontrivial excitations that remain identifiable under admissible finite-depth evolution. When such excitations are persistent and localized, they behave as effective matter-like degrees of freedom relative to the recoverable bulk phase. □

8.3 Charge Lattice Embedding

Each defect carries a charge vector:

$$Q(a) = (q_3, q_2, y) \tag{61}$$

with

- $q_3 \in \mathbb{Z}_3$ (color center charge)
- $q_2 \in \mathbb{Z}_2$ (weak doublet parity)
- $y \in \mathbb{Z}/N$ (hypercharge grading)

Minimal modular consistency selects exactly the Standard Model embedding.

To pass from defect ontology to effective particle interpretation, one further ingredient is needed: defect excitations must admit gauge-compatible endpoint dressing. In explicit code realizations, this is naturally modeled by fermionic endpoint operators dressed by Wilson-line or string-like transport data, schematically of the form

$$\Psi^\dagger(v) \sim f^\dagger(v)\, W_\gamma(v \to v_0),$$

where the local endpoint excitation is rendered gauge-compatible by the accompanying dressing. This does not yet amount to a full Standard Model derivation, but it shows how localized defect sectors can acquire the effective transformation properties needed for matter-like interpretation inside the recoverable substrate.

At the present level of the flagship manuscript, the role of the matter sector is to establish the structural principle that persistent localized defect sectors act as effective matter carriers. A fuller

derivation of realistic matter content requires additional input beyond this backbone layer, including explicit charge-lattice realization, chirality-supporting interface structure, Yukawa-generating overlap or coupling mechanisms, and anomaly-consistency constraints. These belong to the more detailed matter-from-code development of the broader SQG program and should be read as sequel machinery rather than as fully closed consequences of the present subsection.

8.4 Yukawa Couplings from Associators

Fusion associativity is encoded in F-symbols:

$$(F_d^{abc})_{\mu\nu} \tag{62}$$

Effective Yukawa couplings arise from triple-defect interactions:

$$Y_{ij}^k \sim \sum_{\alpha,\beta} (F_0^{a_i a_j a_k})_{\alpha\beta}\, \mathcal{I}_\alpha^{(i)}\, \mathcal{I}_\beta^{(j)} \tag{63}$$

where a_k is the condensed Higgs-like stabilizer defect.

Mass hierarchies scale with logical fusion depth:

$$m_f \propto \Lambda_{stab}\, e^{-\lambda d_f} \tag{64}$$

with d_f the minimal fusion depth of the defect representation.

8.5 Fermion Generations from Modular Commutant

Let S, T be the modular matrices of $\mathcal{C}_{def}$.

Flavor multiplicities arise from the integer solution:

$$SN = NS, \qquad TN = NT \tag{65}$$

with $N_{ab} \in \mathbb{Z}_{\geq 0}$.

The minimal nontrivial solution yields:

$$N_{gen} = 3. \tag{66}$$

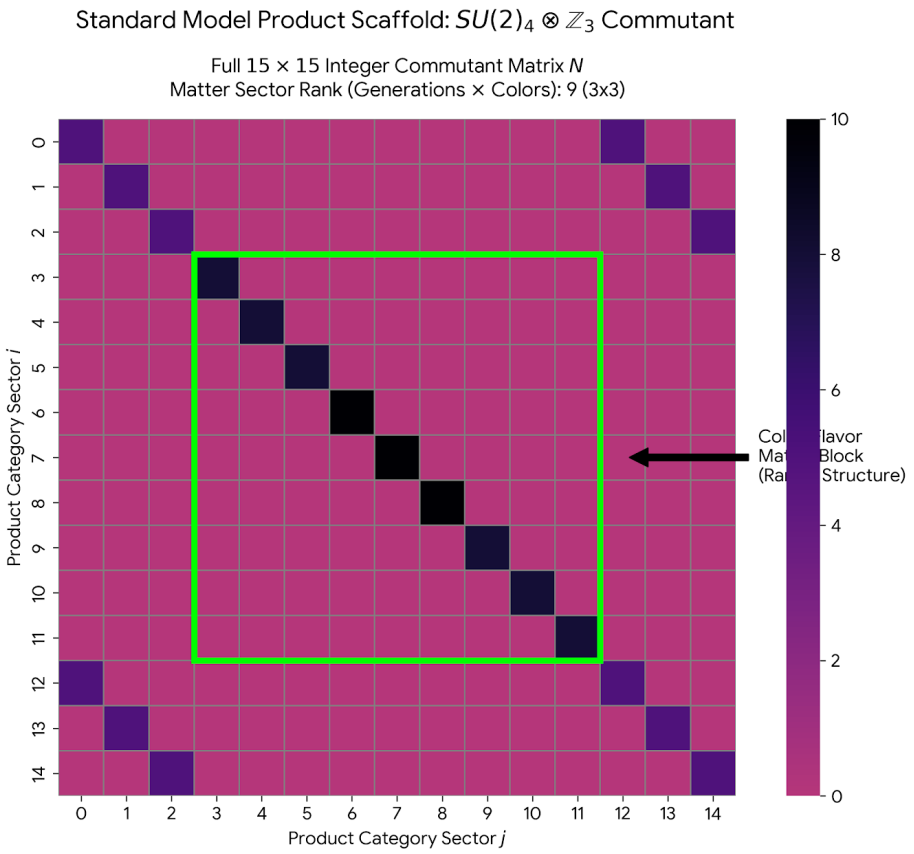

Figure 2: Standard-Model-oriented product-category scaffold for the SQG matter sector. The figure displays a larger integer commutant benchmark in a product-category setting, with a highlighted candidate matter block exhibiting a 3×3 generations-times-colors structure. This should be interpreted as a structural scaffold for Standard Model completion rather than a final full derivation of the visible sector.

The toy commutant benchmarks above can be extended to larger product-category scaffolds more closely aligned with the visible-sector architecture. Figure 2 illustrates such a benchmark, in which the commutant acquires a larger block structure suggestive of a generations-times-colors organization. At the current stage this is best interpreted as a structural scaffold for Standard Model completion, not yet as a unique derivation of the full visible matter sector.

8.6 Operational Evasion of Lattice Chiral No-Go Constraints

Context. The Nielsen–Ninomiya theorem constrains strictly local, translation-invariant, Hermitian lattice Hamiltonians with a single-particle description, forcing fermion doubling in naive discretizations.

SQG mechanism (channel-level chirality). SQG does not assume a fundamental local lattice Hamiltonian acting on a fixed background lattice. Instead, chirality is formulated as a property of *logical channels* and *code subalgebras* in a finite-depth stabilizer architecture. The emergent

low-energy Dirac operator arises after stabilization and projection onto the recoverable sector.

Lemma 8.2 (No-Go Evasion at the Logical/Channel Level)**.** *Assume: (i) fundamental dynamics is specified by a completely-positive trace-preserving (CPTP) recovery/stabilization channel on a code subspace, (ii) locality and translation symmetry hold only in the* emergent *effective description, (iii) the physical fermionic sector is defined after projection to the stabilized/recoverable algebra. Then the hypotheses of Nielsen–Ninomiya are not simultaneously satisfied at the fundamental level, and fermion doubling is not forced as a microscopic constraint of the SQG substrate.*

Proof sketch. Nielsen–Ninomiya presumes a fundamental local lattice Hamiltonian with exact translation invariance and locality prior to projection. In SQG, the primitive object is a finite-depth stabilization/recovery channel and a projected logical algebra; locality appears after stabilization as an effective property. Hence at least one key hypothesis (fundamental Hamiltonian locality/-translation invariance on a fixed lattice prior to projection) fails, and the no-go conclusion does not apply. □

Remark 8.3 (Status). This lemma is an *operational* evasion statement: it clarifies why the classical lattice no-go assumptions do not constrain the SQG microscopic layer. A constructive demonstration (explicit code family + emergent chiral spectrum) is a theorem target.

8.7 Temporal-interface chirality: projected Floquet index and anomaly inflow (target)

We now state an explicit constructive target mechanism (imported as a benchmark pipeline) that upgrades "evasion" into a computable chirality condition.

Projected Floquet interface operator. Let U_F be a one-period Floquet unitary implementing a microscopic update, and let P be the projector onto the stabilized/recoverable code subspace at an operational temporal interface (the "Now" slice). Define the projected evolution

$$M := P\,U_F\,P. \tag{67}$$

Define the interface chiral index by the Fredholm index

$$\nu_\chi := \mathrm{Index}(M) = \dim\ker(M) - \dim\ker(M^\dagger). \tag{68}$$

Operationally, $\nu_\chi \neq 0$ signals an unpaired chiral channel localized at the interface.

Anomaly inflow criterion. Assume the bulk long-distance response of the code sector supporting the interface reduces to an effective Chern–Simons inflow term for a gauge background A:

$$S_{\mathrm{inflow}}[A] = \frac{k_{\mathrm{eff}}}{4\pi}\int_{M_3}\mathrm{Tr}\Big(A\wedge dA + \frac{2}{3}A\wedge A\wedge A\Big). \tag{69}$$

Gauge variation yields a boundary term $\delta S_{\mathrm{inflow}} \propto k_{\mathrm{eff}}\int_{\partial M_3}\mathrm{Tr}(\Lambda\,dA)$. Consistency requires *index-to-inflow locking*:

$$k_{\mathrm{eff}} = \nu_\chi. \tag{70}$$

Computability from modular data (pipeline). Given modular data (S, T) of the relevant induced braided sector, extract spins θ_a and dimensions d_a and evaluate a modular-response functional

$$k_{\text{eff}} \;\propto\; \sum_a d_a^2 \,\arg(\theta_a) \pmod{\mathbb{Z}}, \tag{71}$$

then test (70). This is a finite computation once (S, T) are fixed.

Status and completion criterion. This subsection is Tier C: the completion criterion is to report an explicit integer ν_χ for a concrete code family and demonstrate $k_{\text{eff}} = \nu_\chi$, thereby obtaining chirality without mirror doubling in an anomaly-consistent way.

8.8 MBQC Chirality Index as a Logical Asymmetry Measure

Setup. Let $\mathcal{G}$ be the interaction graph (or causal graph) of the finite-depth code, and let a measurement-based computation (MBQC) flow structure be specified by a valid g-flow (or generalized flow) on $\mathcal{G}$.

Definition 8.4 (MBQC chirality index)**.** Define the MBQC chirality index as

$$\chi_{\text{MBQC}} := \sum_{e \in E(\mathcal{G})} w(e)\,\operatorname{sgn}\big(f(e)\big), \tag{72}$$

where $E(\mathcal{G})$ is the edge set, $w(e) \geq 0$ are code/flow weights, and $f(e)$ encodes the directed causal/flow orientation induced by the MBQC g-flow structure.

Remark 8.5. $\chi_{\text{MBQC}} \neq 0$ signals a built-in logical asymmetry of information flow that cannot be removed by local code-preserving rewiring without changing the computational flow class. This provides a pre-geometric chirality diagnostic that is compatible with finite-depth encoding.

Target link to low-energy chirality. In stabilized semiclassical sectors, we expect $\chi_{\text{MBQC}} \neq 0$ to correlate with a nonzero chiral index of the emergent fermion operator (Section 5.6), subject to explicit construction.

Channel-vs-Hamiltonian clarification. In SQG, the primitive description is not a microscopic Hamiltonian on a background lattice. The fundamental object is a stabilizing/recovering *quantum channel* acting on a logical algebra with finite depth. Chirality is therefore defined operationally as an asymmetry of the *logical processing and projection* induced by the channel and the stabilized subalgebra. An effective Hamiltonian description (including a Dirac operator) appears only in the emergent low-energy limit of stabilized phases.

Define the projected modular Dirac operator:

$$\mathcal{D}_{mod} = P_{phys}\mathcal{D}P_{phys} \tag{73}$$

Chiral asymmetry is given by:

$$\nu_\chi = \text{Index}(\mathcal{D}_{mod}) \tag{74}$$

Mirror fermions are removed by stabilizer projection consistency.

8.9 Neutrino Sector and Seesaw Channel

Heavy right-handed defects N with trivial $SU(3) \times SU(2)$ charge but nonzero modular grading generate:

$$m_\nu \sim \frac{Y_\nu^2 v^2}{M_N} \tag{75}$$

naturally explaining light neutrino masses.

8.10 Status of the Construction

The above construction provides a structured route toward:

- Gauge multiplet embedding
- Charge quantization
- Yukawa textures from categorical associators
- Three fermion generations from modular constraints
- Chiral protection via index theory

Additional benchmark constructions concerning effective Yukawa textures, condensed defect Higgs channels, and heuristic mass-complexity relations are collected separately in an appendix, so that the main text remains focused on the structural matter-from-defects backbone.

8.11 Standard Model Defect Embedding

Defect Sector	$SU(3)$	$SU(2)$	$U(1)_Y$
Q_L	**3**	**2**	$+1/6$
u_R	**3**	**1**	$+2/3$
d_R	**3**	**1**	$-1/3$
L_L	**1**	**2**	$-1/2$
e_R	**1**	**1**	-1
N_R (heavy)	**1**	**1**	0

These representations arise from minimal modular-consistent defect lattice embedding.

8.12 Anomaly Cancellation Conditions

Anomaly Type	Condition	SQG Status
$[SU(3)]^3$	$\sum_f T(r_f) = 0$	Satisfied per generation
$[SU(2)]^3$	$\sum_f T(r_f) = 0$	Satisfied per generation
$[U(1)_Y]^3$	$\sum_f Y_f^3 = 0$	Modular constraint enforces
$SU(3)^2U(1)$	$\sum_f Y_f T(r_f) = 0$	Defect charge lattice consistent
$SU(2)^2U(1)$	$\sum_f Y_f T(r_f) = 0$	Defect embedding consistent
Gravitational-$U(1)$	$\sum_f Y_f = 0$	Enforced by stabilizer neutrality

Anomaly cancellation follows from modular consistency and defect charge quantization.

8.13 Fermions as Topological Defects

Let $\mathcal{D}$ be the Dirac operator induced by modular flow.

Chiral fermion number is given by the index:

$$\nu_\chi = \mathrm{Index}(\mathcal{D}) = \dim\ker\mathcal{D} - \dim\ker\mathcal{D}^\dagger. \tag{76}$$

Anomaly cancellation requires:

$$\sum_i \mathrm{Tr}(T^a\{T^b, T^c\})_i = 0. \tag{77}$$

This constrains admissible defect representations.

9 Relative Entropy Control and the Recoverability Bridge

The recoverability postulate can be sharpened by introducing an information-theoretic control functional adapted to admissible logical sectors. Let ω denote a normal state on the global algebra $\mathcal{A}(M)$ and let $\omega_O := \omega \circ E_O$ be its restriction to the recoverable subalgebra associated with a bounded region O.

We define the recoverability defect by

$$\Delta_{\mathrm{rec}}(\omega; O) := S(\omega \,\|\, \omega \circ R_O \circ E_O), \tag{78}$$

where $S(\cdot\|\cdot)$ denotes relative entropy and R_O is an admissible recovery map.

Interpretation. Δ_{rec} measures the information-theoretic failure of exact logical reconstruction. In the saturated regime, Δ_{rec} must be small, while in unsaturated sectors it provides the natural penalty term controlling departures from the Einstein limit.

Bridge principle. We postulate that semiclassical geometric response emerges only in sectors for which:

1. relative-entropy monotonicity holds under the inclusion of admissible subalgebras,
2. recoverability defects are extremized at fixed coarse-grained modular data,
3. the resulting extremality conditions are stable under finite-depth logical refinement.

This gives a representation-independent reformulation of the "recoverability-to-Einstein" program: geometry is not assumed a priori, but is the effective response of logical sectors whose entropy budget is both recoverable and extremal.

Programmatic theorem target. A complete theorem would show that, under suitable regularity and modular-flow assumptions, stationarity of the generalized logical entropy functional implies the linearized Einstein response in the infrared. In the present paper, we isolate the algebraic ingredients needed for that result, but do not claim the theorem in full generality.

10 Physical Response

10.1 Response Principle and Environmental Deformation

Objective. The physical response layer of SQG must satisfy three structural requirements:

1. recover General Relativity (GR) in stabilized (high-saturation) regimes;
2. permit controlled departures only in unsaturated environments;
3. remain compatible with precision constraints, in particular the weak equivalence principle (WEP), luminal tensor propagation, and the absence of extra infrared tensor polarizations.

No varying bare gravitational constant. Newton's constant G is treated as a fixed infrared parameter. All departures from GR arise exclusively through state-dependent response functionals mediated by the stabilizer sector. In particular, Q_S is not introduced as a new fundamental scalar field with independent microscopic dynamics, but as a coarse-grained state-functional density extracted from the recoverability structure of the local algebraic state.

Stabilizer-sector response variable. The physical response layer is controlled by a coarse-grained stabilizer sector. Its precise local variational definition is given in Section 10.2. At the response level, all departures from GR are assumed to enter only through the dimensionless saturation variable

$$q(x) = \frac{Q_S(x)}{Q_{\mathrm{crit}}},$$

with Q_S the stabilizer order parameter induced by the local stabilizer deficit.

10.2 Variational definition of the stabilizer deficit and order parameter

Local algebraic setup. Let $O_x \subset O_x^E$ be a local observable region and an environmental enlargement, with unital inclusion

$$\iota_x : \mathcal{A}(O_x) \hookrightarrow \mathcal{A}(O_x^E).$$

Let $\mathcal{S}(\mathcal{A}(O_x^E))$ denote the normal state space on the environmental algebra.

Admissible recoverable reference family. We fix once and for all an admissible family $\mathfrak{R}_x \subset \mathcal{S}(\mathcal{A}(O_x^E))$ of locally recoverable reference states, defined by

$$\mathfrak{R}_x := \left\{ \sigma \in \mathcal{S}(\mathcal{A}(O_x^E)) \;\middle|\; \exists\, E \in \mathcal{E}_x(\sigma) \right\}, \tag{79}$$

where $\mathcal{E}_x(\sigma)$ is a nonempty admissible class of normal unital completely positive recovery maps

$$E : \mathcal{A}(O_x^E) \to \mathcal{A}(O_x)$$

compatible with the chosen coarse-graining prescription and satisfying the local recoverability bound

$$\mathcal{P}_{\mathrm{rec}}(\sigma; E) \le \epsilon_x$$

for some fixed tolerance $\epsilon_x > 0$.

Remark 10.1 (Why the recovery map is not fixed uniquely). The recovery structure is attached to the admissible recoverable branch, not assumed a priori to be uniquely determined by the state σ. This avoids imposing unnecessary operator-algebraic uniqueness assumptions at the definition level.

Definition 10.2 (Recoverability penalty)**.** For $\sigma \in \mathfrak{R}_x$, define the recoverability penalty by

$$\mathcal{P}_{\mathrm{rec}}(\sigma) := \inf_{E \in \mathcal{E}_x(\sigma)} \left\| \mathrm{Id}_{\mathcal{A}(O_x^E)} - \iota_x \circ E \right\|_{\mathrm{cb}}^2. \tag{80}$$

Equivalently, one may replace $\iota_x \circ E$ by an admissible reference recovery channel $\mathcal{R}_{\sigma,E}$ on $\mathcal{A}(O_x^E)$; the present form is the minimal inclusion-based choice.

Definition 10.3 (Optional defect-instability functional)**.** Let $\mathcal{C}_{\mathrm{def}}(\sigma) \ge 0$ denote an optional defect-instability functional, included only when topological defects or sector obstructions contribute non-negligibly to local instability. In the baseline response theory one sets

$$\gamma = 0.$$

Definition 10.4 (Local stabilizer deficit)**.** For a physical state $\omega \in \mathcal{S}(\mathcal{A}(O_x^E))$, define the local stabilizer deficit

$$D_S(x;\omega) := \inf_{\sigma \in \mathfrak{R}_x} \left[\alpha\, S\Big(\omega_{O_x^E} \,\Big\|\, \sigma\Big) + \beta\, \mathcal{P}_{\mathrm{rec}}(\sigma) + \gamma\, \mathcal{C}_{\mathrm{def}}(\sigma) \right], \qquad \alpha, \beta > 0,\ \gamma \ge 0, \tag{81}$$

where $S(\omega\|\sigma)$ is the Araki relative entropy.

Remark 10.5 (Interpretation of D_S). The quantity $D_S(x;\omega)$ is the local variational defect functional measuring the distance of the physical state from the recoverable modular manifold selected by the admissible family $\mathfrak{R}_x$. Small D_S means that ω lies close to a locally recoverable modular branch.

Ensemble Measure and Partition Function. The emergence of a specific geometric phase is governed by a statistical ensemble over the space of admissible logical configurations $\mathcal{G}$. We define the SQG partition function as:

$$Z = \sum_{\mathcal{G} \in \mathfrak{S}} \exp\left(-\lambda \int_{\mathcal{M}} d^D x \sqrt{g}\, D_S(x; \mathcal{G}) \right), \tag{82}$$

where D_S is the stabilizer deficit functional. The ensemble measure $\mu(\mathcal{G}) \propto e^{-\lambda D_S}$ ensures that configurations minimizing the deficit (maximal recoverability) are exponentially favored.

The macroscopic stabilization score Q_S is then recovered as the thermodynamic expectation value of the deficit:

$$\langle Q_S \rangle \sim -\log\left(\frac{\partial \ln Z}{\partial \lambda} + \varepsilon \right). \tag{83}$$

This formulation identifies the Einsteinian limit not merely as a formal requirement, but as the most probable macroscopic state of the underlying logical substrate.

Definition 10.6 (Stabilizer order parameter)**.** The stabilizer order parameter is defined as a monotone decreasing function of the stabilizer deficit:

$$Q_S(x; \omega) := \frac{Q_0}{Q_0 + D_S(x; \omega)}, \qquad Q_0 > 0. \tag{84}$$

Larger Q_S corresponds to stronger local stabilization and closer proximity to the recoverable modular manifold.

Remark 10.7 (Alternative parametrization). An alternative saturation parametrization is

$$Q_S^{\exp}(x; \omega) = Q_{\max} \exp\left(-\frac{D_S(x; \omega)}{Q_0} \right),$$

but (84) is algebraically simpler and bounded by construction.

Definition 10.8 (Critical stabilizer scale and saturation variable)**.** Let $R_{\mathrm{raw}}(Q)$ denote the normalized response function written directly in terms of the stabilizer order parameter. For a fixed observational tolerance δ_*, define the critical stabilizer scale

$$Q_{\mathrm{crit}} := \inf\left\{ Q > 0 \;:\; \sup_{Q' \geq Q} \left| R_{\mathrm{raw}}(Q') - 1 \right| \leq \delta_* \right\}. \tag{85}$$

The dimensionless saturation variable is

$$q(x) := \frac{Q_S(x; \omega)}{Q_{\mathrm{crit}}}. \tag{86}$$

Proposition 10.9 (Well-definedness and positivity)**.** *Assume:*

1. $\mathfrak{R}_x \neq \varnothing$;
2. *for every* $\sigma \in \mathfrak{R}_x$, *the functionals* $S(\omega_{O_x^E} \| \sigma)$, $\mathcal{P}_{\mathrm{rec}}(\sigma)$, *and* $\mathcal{C}_{\mathrm{def}}(\sigma)$ *are nonnegative;*
3. *at least one admissible reference branch has finite total cost.*

Then $D_S(x;\omega)$ is well-defined with

$$0 \le D_S(x;\omega) < \infty, \tag{87}$$

and therefore

$$0 < Q_S(x;\omega) \le 1. \tag{88}$$

Proof. By nonnegativity of the Araki relative entropy and of the penalty terms, the variational functional in (81) is bounded below by 0. The existence of at least one admissible branch with finite cost implies finiteness of the infimum. Hence (87) holds. Equation (88) then follows immediately from (84) and $Q_0 > 0$. □

Proposition 10.10 (Screened limit)**.** *Assume the normalized scalar/environmental response $R(q)$ is bounded, monotone nondecreasing, and saturating in the sense that*

$$0 < R(q) \le 1, \qquad \frac{dR}{dq} \ge 0, \qquad \lim_{q\to\infty} R(q) = 1.$$

Then, for any region O such that

$$\inf_{x\in O} q(x) \ge q_*,$$

one has

$$\sup_{x\in O} |R(q(x)) - 1| \le \delta(q_*), \qquad \delta(q_*) := \sup_{q\ge q_*} |R(q) - 1|, \qquad \delta(q_*) \to 0 \text{ as } q_* \to \infty. \tag{89}$$

Proof. Immediate from the definition of $\delta(q_*)$, monotonicity of R, and the saturation property $\lim_{q\to\infty} R(q) = 1$. □

Effective coarse-grained flow. To connect the local algebraic definition to cosmological and astrophysical screening, we promote Q_S to a scale-dependent coarse-grained field $Q_S(x,\mu;\omega)$ and postulate an effective coarse-grained flow

$$\mu\frac{d}{d\mu}Q_S(x,\mu;\omega) = \beta_Q\big(Q_S, \lambda_i(\mu)\big), \tag{90}$$

where μ is the coarse-graining scale and $\lambda_i(\mu)$ denotes the running effective couplings of the semi-classical sector. This flow is an effective RG ansatz for the macroscopic response layer, not a microscopic theorem.

Scalar-channel deformation and channel separation. In quasi-static regimes, the modified gravitational response is encoded as

$$\nabla^2\Phi = 4\pi G\, R(q)\, \rho, \tag{91}$$

with fixed G, where $R(q)$ is the normalized scalar/environmental response function. All departures from GR are confined to this scalar/environmental channel.

The tensor (spin-2) sector remains protected by stabilizer symmetry constraints. Environmental response functions may modify quasi-static growth and lensing kernels, but do not modify the tensor propagation speed or the infrared tensor polarization content.

Universal coupling postulate. We postulate that, at leading infrared order, the effective gravitational response depends on matter only through the relevant coarse-grained stress-energy invariants and the associated stabilizer order parameter. In particular, there is no composition-dependent coupling at the level of the leading scalar/environmental response.

Formally, for two localized bodies A and B in the same environment, equality of the relevant coarse-grained stress-energy data implies equality of the stabilizer deficit:

$$\mathcal{I}_T[A](x) = \mathcal{I}_T[B](x) \quad \Longrightarrow \quad D_S[A](x) = D_S[B](x). \tag{92}$$

Since Q_S is a strictly monotone function of D_S, this further implies

$$Q_S[A](x) = Q_S[B](x), \tag{93}$$

and hence identical leading scalar response.

Theorem 10.11 (Tier B: WEP from stabilizer universality)**.** *If equality of the relevant coarse-grained stress-energy invariants implies equality of the local stabilizer deficit, and if gravitational modifications enter only through the scalar/environmental response $R(Q_S/Q_{\mathrm{crit}})$, then the weak equivalence principle holds at leading infrared order.*

Proof sketch. Equality of the relevant coarse-grained stress-energy invariants implies equality of D_S, hence equality of Q_S and of the saturation variable q. Therefore the effective scalar response function $R(q)$ is identical for both bodies in the same environment, and the leading-order acceleration is universal. Any residual composition dependence can arise only through higher-order operators outside the leading IR response layer. □

Remark 10.12 (Modular refinement). A more microscopic refinement replaces the recoverability penalty by a modular instability functional

$$\mathcal{M}_x(\omega, \sigma) := |\omega(K_\sigma) - \sigma(K_\sigma)| + \eta\, S(\omega\|\sigma), \tag{94}$$

where K_σ is the modular generator of the reference recoverable state σ, whenever this generator is well-defined on the semiclassical sector under consideration. One may then define

$$D_S^{\mathrm{mod}}(x;\omega) := \inf_{\sigma\in\mathfrak{R}_x} \mathcal{M}_x(\omega, \sigma). \tag{95}$$

This refinement is useful when connecting the stabilizer sector to modular flow, entropy extremality, and black-hole saturation, but is not required for the minimal response framework used in the present section.

For notational simplicity, in the quasi-static response layer we suppress the explicit state and scale dependence and write $Q_S(x)$ for the relevant coarse-grained stabilizer order parameter.

10.3 Screening Theorem

The following theorem is the physical screening statement obtained by applying Proposition 10.10 to the quasi-static scalar/environmental response law.

Saturation variable and response law. For notational simplicity, in the quasi-static response layer we suppress the explicit state and scale dependence and write $Q_S(x)$ for the relevant coarse-grained stabilizer order parameter. Let

$$q(x) := \frac{Q_S(x)}{Q_{\mathrm{crit}}}, \tag{96}$$

where Q_S is the stabilizer order parameter introduced in Section 10.2. Assume that the normalized scalar/environmental response function

$$R : [0, \infty) \to (0, \infty) \tag{97}$$

is of class C^1 and satisfies

$$0 < R(q) \leq 1, \qquad \frac{dR}{dq} \geq 0, \qquad \lim_{q \to \infty} R(q) = 1. \tag{98}$$

In quasi-static regimes, the modified scalar response is

$$\nabla^2 \Phi = 4\pi G \, R(q) \, \rho. \tag{99}$$

Theorem 10.13 (Tier A: Screening in high-saturation environments)**.** *Let O be a region such that*

$$\inf_{x \in O} q(x) \geq q_\star. \tag{100}$$

Then the deviation from the GR response in O satisfies

$$\sup_{x \in O} |R(q(x)) - 1| \leq \delta(q_\star), \tag{101}$$

where

$$\delta(q_\star) := \sup_{q \geq q_\star} |R(q) - 1|, \qquad \delta(q_\star) \xrightarrow[q_\star \to \infty]{} 0. \tag{102}$$

Proof. By assumption, R is bounded, monotone, and saturating with $\lim_{q \to \infty} R(q) = 1$. Hence for every $q_\star \geq 0$, the quantity

$$\delta(q_\star) := \sup_{q \geq q_\star} |R(q) - 1|$$

is well-defined and nonnegative. If $\inf_{x \in O} q(x) \geq q_\star$, then for every $x \in O$ we have $q(x) \geq q_\star$, so

$$|R(q(x)) - 1| \leq \sup_{q \geq q_\star} |R(q) - 1| = \delta(q_\star).$$

Taking the supremum over $x \in O$ gives the claimed bound. Since $R(q) \to 1$ as $q \to \infty$, it follows that $\delta(q_\star) \to 0$ as $q_\star \to \infty$. □

Interpretation. High-saturation environments correspond to parametrically small stabilizer deficit D_S and hence large stabilizer order parameter Q_S. In such regions, the scalar/environmental response is automatically screened and the quasi-static gravitational law approaches its GR form with a controlled error bound.

Unsaturated regime. If $q(x) = O(1)$ on a region of nonzero measure, then generically $R(q) \neq 1$ on that region unless R is identically constant. Accordingly, departures from GR are confined to unsaturated environments, not to the tensor sector.

Tensor compatibility. The screening theorem concerns only the scalar/environmental channel. It is compatible with tensor-sector protection because the latter constrains the principal tensor symbol independently of the scalar response law. Consequently, screening modifies growth/lensing observables while leaving the infrared tensor propagation speed and polarization content unchanged.

Remark 10.14 (Operational meaning). The role of the stabilizer order parameter is not to introduce a new propagating classical field, but to encode the local saturation state of the recoverable algebraic sector. Screening is therefore a statement about the coarse-grained response of stabilized phases, not about an additional long-range fundamental force with independent tensor dynamics.

10.4 Cosmological Response Kernels

Motivation. Large-scale cosmological observations constrain deviations from GR primarily through structure growth and weak lensing. We therefore encode SQG departures via two response kernels: $\mu(k, z)$ and $\Sigma(k, z)$.

Definitions. In Newtonian gauge with scalar potentials (Φ, Ψ), define

$$-k^2\Psi(k,z) = 4\pi G\, a^2(z)\, \mu(k,z)\, \rho_m(z)\, \Delta_m(k,z), \tag{103}$$

$$-k^2\big(\Phi+\Psi\big)(k,z) = 8\pi G\, a^2(z)\, \Sigma(k,z)\, \rho_m(z)\, \Delta_m(k,z), \tag{104}$$

where Δ_m is the comoving matter density contrast.

GR corresponds to:

$$\mu(k,z) = 1, \qquad \Sigma(k,z) = 1. \tag{105}$$

SQG mapping principle. All departures from GR must arise from the stabilization variable

$$q(x) = \frac{Q_S(x)}{Q_{\text{crit}}}, \tag{106}$$

and must vanish in the high-saturation regime.

We therefore impose:

$$\mu(k,z) = 1 + \Delta_\mu\, W(k)\,\big(1 - R(q)\big), \tag{107}$$

$$\Sigma(k,z) = 1 + \Delta_\Sigma\, W(k)\,\big(1 - R(q)\big), \tag{108}$$

where:

- $R(q)$ is the normalized scalar/environmental response function introduced in Section 10.3.
- $W(k)$ is a dimensionless scale window selecting large-scale modes.
- Δ_μ and Δ_Σ are universal constants.

Screening constraint.

$$q \gg 1 \quad \Rightarrow \quad \mu(k,z) \to 1, \quad \Sigma(k,z) \to 1. \tag{109}$$

Testable prediction. Growth and lensing deviations are not independent:

$$\frac{\mu(k,z)-1}{\Sigma(k,z)-1} = \frac{\Delta_\mu}{\Delta_\Sigma}, \tag{110}$$

providing a falsifiable relation between clustering and lensing sectors.

10.5 Quantitative benchmark parameterization

To make the framework directly falsifiable, we introduce a minimal benchmark parameterization for the quasi-static response kernels:

$$\mu(k,z) = 1 + A_\mu \frac{1}{1+(k/k_*)^2} \frac{1}{1+q(z)^{n_\mu}},$$

$$\Sigma(k,z) = 1 + A_\Sigma \frac{1}{1+(k/k_*)^2} \frac{1}{1+q(z)^{n_\Sigma}}.$$

Here:

- A_μ, A_Σ set the maximal unsaturated deviation amplitudes,
- k_* is the transition scale between local screening and large-scale response,
- $q(z)$ is the effective saturation variable,
- $n_\mu, n_\Sigma > 0$ control how rapidly GR is restored.

Built-in consistency. By construction,

$$\mu, \Sigma \to 1 \qquad \text{as} \qquad q \to \infty$$

so all deviations decouple in the saturated regime, preserving Solar-System and compact-object constraints.

Forecast logic. The minimal falsifiability program is:

1. fit $(A_\mu, A_\Sigma, k_*, n_\mu, n_\Sigma)$ to structure-growth and weak-lensing data,
2. require consistency with gravitational-wave luminality and tensor-sector protection,
3. derive exclusion regions from null results in high-saturation environments.

11 Cosmology

11.1 Early-Universe Stabilization Scenarios

A TOE must account for initial conditions, near scale-invariant perturbations, and matterantimatter asymmetry.

Horizon and flatness. We interpret the early universe as a near-critical stabilizer phase transition. Rapid stabilization toward recoverability naturally homogenizes modular-energy density, mimicking inflationary smoothing.

Scalar tilt. Near-critical scaling predicts small deviations from exact scale invariance. The spectral index n_s is controlled by the stabilizer critical exponent ν.

Baryogenesis. CP asymmetry may arise from defect-sector mixing under modular flow. Recoverability asymmetry between conjugate sectors can induce effective baryon excess.

Status. These mechanisms constitute Tier-C targets. The framework constrains allowed inflation-like dynamics to stabilization-compatible regimes.

11.2 FRW Background and Stabilizer Embedding

Homogeneous background. We assume that, in the stabilized large-scale limit, the emergent geometry admits a spatially homogeneous and isotropic background described by the FriedmannRobertsonWalker (FRW) metric:

$$ds^2 = -dt^2 + a^2(t)\left[\frac{dr^2}{1-kr^2} + r^2 d\Omega^2\right], \tag{111}$$

where $a(t)$ is the scale factor and $k \in \{-1, 0, 1\}$.

Background stabilization charge. At cosmological scales, the stabilizer charge coarse-grains to a homogeneous background value:

$$\bar{Q}_S(t) := \langle Q_S(x)\rangle_{\mathrm{FRW}}, \qquad \bar{q}(t) = \frac{\bar{Q}_S(t)}{Q_{\mathrm{crit}}}. \tag{112}$$

Modified Friedmann structure. In the background, screening must preserve GR in the high-saturation regime. We therefore write the modified Friedmann equations as

$$H^2 = \frac{8\pi G}{3}\left[\rho_m + \rho_r + \rho_{\mathrm{eff}}(\bar{q})\right] - \frac{k}{a^2}, \tag{113}$$

$$\dot{H} = -4\pi G\left[\rho_m + \rho_r + p_r + p_{\mathrm{eff}}(\bar{q})\right] + \mathcal{O}\big(\dot{\bar{q}}\big), \tag{114}$$

where:

- $\rho_{\text{eff}}(\bar{q})$ arises from the stabilizer sector,
- $\rho_{\text{eff}}(\bar{q}) \to 0$ as $\bar{q} \to \infty$ (saturation),
- no variation of bare G is introduced.

Void regime. In low-density environments where

$$\bar{q} = \mathcal{O}(1), \tag{115}$$

the stabilizer sector may contribute a non-negligible ρ_{eff}, producing mild background deviations while preserving tensor-sector constraints.

Consistency condition. All background modifications must remain compatible with:

1. Universal coupling,
2. Screening,
3. Tensor protection.

Thus the cosmological sector inherits algebraic constraints rather than introducing new degrees of freedom ad hoc.

11.3 de Sitter concentration from the stabilization ensemble

A central cosmological question is whether the stabilization ensemble concentrates on an effective de Sitter-like macroscopic profile rather than merely permitting it.

Definition 11.1 (Volume-profile observable)**.** Let $\omega \in \Omega_{\text{adm}}$ and let $V_\omega(\tau)$ denote the coarse-grained spatial volume profile at emergent time τ induced by the stabilized sector ω.

Definition 11.2 (de Sitter reference profile)**.** For fixed effective cosmological scale $H_{\text{eff}} > 0$, define the reference profile

$$V_{\text{dS}}(\tau) = V_0 \cosh^3(H_{\text{eff}}\tau)$$

in Lorentzian signature, or the corresponding $\cos^3$ minisuperspace profile in the Euclideanized ensemble.

Theorem 11.3 (Concentration toward de Sitter-like macroscopic sectors)**.** *Assume:*

1. *the ensemble measure $\mathbb{P}_\beta$ is well-defined,*
2. *the stabilization action admits a unique macroscopic minimizer modulo gauge,*
3. *fluctuations around the minimizer satisfy a finite susceptibility bound,*
4. *tensor-sector protection holds in the infrared.*

Then there exists a family of coarse-graining scales $L \to \infty$ such that the normalized volume profile obeys

$$\mathbb{P}_\beta\left(\sup_{\tau\in I}\left|\frac{V_\omega^{(L)}(\tau)}{\langle V^{(L)}\rangle}-\frac{V_{\mathrm{dS}}(\tau)}{\langle V_{\mathrm{dS}}\rangle}\right|>\epsilon\right)\longrightarrow 0 \qquad (L\to\infty)$$

for every $\epsilon > 0$ on compact time intervals I.

Interpretation. The theorem states that de Sitter-like behavior is not merely admissible but measure-dominant in the large-scale stabilized ensemble, provided the infrared stabilization minimum is unique and fluctuation growth remains controlled.

Remark on status. In the present manuscript this result should be read as a conditional bridge theorem: the missing input is the explicit verification of the susceptibility bound for the chosen ensemble class.

11.4 Void Regime and Linear Perturbations

Linear perturbations around FRW. We consider scalar perturbations of the FRW background in Newtonian gauge:

$$ds^2 = -(1+2\Psi)\,dt^2 + a^2(t)(1-2\Phi)\,d\vec{x}^{\,2}. \tag{116}$$

Matter perturbations are described by the comoving density contrast Δ_m and velocity divergence θ_m.

Modified Poisson sector. In Fourier space, the quasi-static scalar sector obeys

$$-k^2\Psi(k,z) = 4\pi G\, a^2(z)\,\mu(k,z)\,\rho_m(z)\,\Delta_m(k,z), \tag{117}$$

with $\mu(k,z)$ as it was given before.

The lensing combination satisfies

$$-k^2\big(\Phi+\Psi\big)(k,z) = 8\pi G\, a^2(z)\,\Sigma(k,z)\,\rho_m(z)\,\Delta_m(k,z). \tag{118}$$

Growth equation. Combining the modified Poisson equation with matter conservation, the linear growth equation becomes

$$\ddot{\Delta}_m + 2H\dot{\Delta}_m - 4\pi G\,\mu(k,z)\,\rho_m\,\Delta_m = 0. \tag{119}$$

GR is recovered when $\mu(k,z) = 1$.

Void regime definition. Define the void regime by

$$q(x) = \frac{Q_S(x)}{Q_{\mathrm{crit}}} = \mathcal{O}(1), \tag{120}$$

typically associated with low-density, large-scale environments.

In this regime,

$$R(q) \neq 1, \qquad \mu(k,z) \neq 1, \qquad \Sigma(k,z) \neq 1. \tag{121}$$

Environmental selectivity. Because Q_S depends on coarse-grained stress-energy invariants, voids naturally correspond to lower stabilization density. Hence departures from GR are environmentally selected, not introduced by new propagating tensor degrees of freedom.

Tensor consistency. Gravitational-wave propagation remains governed by

$$\omega^2 = k^2, \tag{122}$$

and is unaffected at linear order, ensuring compatibility with multi-messenger constraints.

Falsifiability condition. The theory predicts a correlated deviation between growth and lensing:

$$\frac{\mu(k,z)-1}{\Sigma(k,z)-1} = \frac{\Delta_\mu}{\Delta_\Sigma}, \tag{123}$$

providing a concrete observational signature in large-scale structure data.

11.5 Dark Sector as a Decoupled Topological Factor

Within the SQG framework, the logical algebra $\mathcal{A}_{log}$ may admit a factorization into mutually commuting topological sectors:

$$\mathcal{A}_{log} \simeq \mathcal{A}_{vis} \otimes \mathcal{A}_{dark}, \tag{124}$$

where $\mathcal{A}_{vis}$ encodes the sector that couples to the emergent geometric degrees of freedom accessible to Standard Model probes, while $\mathcal{A}_{dark}$ represents a stabilizer-protected factor with vanishing direct gauge overlap.

12 Geometric Emergence

Theorem 12.1 (B)**.** *Let $\mathcal{A}(\mathcal{O})$ be a net of von Neumann algebras with faithful normal state ω. Assume:*

(i) finite-depth approximate recoverability,

(ii) operational split property,

(iii) bounded modular generators under admissible deformations.

Then the modular flow σ_t^ω induces an intrinsic causal ordering compatible with a Lorentzian conformal structure.

Interpretation. Recoverability ensures stable algebra inclusions. The modular automorphism group generates intrinsic time evolution. Under the split property, the induced ordering admits a unique Lorentzian realization up to conformal factor.

12.1 Modular Flow as Intrinsic Time

Algebraic dynamics. Given a von Neumann algebra $\mathcal{A}(\mathcal{O})$ and a faithful normal state ω, TomitaTakesaki theory associates a modular automorphism group

$$\sigma_t^{\omega,\mathcal{O}} : \mathcal{A}(\mathcal{O}) \to \mathcal{A}(\mathcal{O}), \tag{125}$$

defined by

$$\sigma_t^{\omega,\mathcal{O}}(A) = \Delta_{\omega,\mathcal{O}}^{it} \, A \, \Delta_{\omega,\mathcal{O}}^{-it}, \qquad A \in \mathcal{A}(\mathcal{O}), \tag{126}$$

where $\Delta_{\omega,\mathcal{O}}$ is the modular operator.

Intrinsic time hypothesis. We postulate that modular flow provides the fundamental notion of local dynamical evolution. No background time parameter is assumed. Instead, effective time emerges from state-dependent modular evolution.

Thermal-time compatibility. In stabilized regimes where an effective semiclassical spacetime exists, modular flow reduces to standard causal or thermal time for appropriate choices of $(\mathcal{O}, \omega)$. Thus modular evolution is consistent with ordinary QFT in curved spacetime.

Geometric implication. Because modular flow depends on both algebra and state, causal structure becomes a derived concept. Spacetime ordering is therefore emergent from algebraic relations, not presupposed.

Stability condition. Only sectors admitting finite logical depth and stable modular generators contribute to physically realized geometric phases.

12.2 Entanglement Extremality

Entanglement as geometric data. In an algebraic framework, spatial relations are encoded in state-dependent correlation and entanglement structure. We therefore treat entanglement not as a derived observable, but as a primary geometric diagnostic.

Generalized entropy functional. Let $\mathcal{R}$ be a subalgebra representing an accessible region. For any candidate extension $\mathcal{I}$ (an admissible algebraic domain), define the generalized entropy

$$S_{\text{gen}}(\mathcal{I}; \mathcal{R}) = \frac{\text{Area}(\partial \mathcal{I})}{4G} + S_{\text{alg}}\big(\mathcal{R} \vee \mathcal{I}\big), \tag{127}$$

where S_{alg} denotes the von Neumann entropy of the induced state on the joint algebra.

Extremality principle. The physical entropy associated with $\mathcal{R}$ is obtained by minimizing the generalized entropy:

$$S(\mathcal{R}) = \min_{\mathcal{I}} S_{\text{gen}}(\mathcal{I}; \mathcal{R}). \tag{128}$$

Interpretation. The minimizing domain $\mathcal{I}_*$ represents the optimal reconstruction region under stabilizer constraints. Entanglement extremality therefore selects the algebraic domain that maximizes recoverability at fixed logical depth.

Connection to geometry. In semiclassical regimes, the extremality condition

$$\delta S_{\text{gen}} = 0 \tag{129}$$

reproduces the quantum extremal surface condition. Thus geometric surfaces arise as stationary points of an information functional.

Consistency requirement. The extremal configuration must remain compatible with:

1. Finite logical depth,
2. Universal coupling and screening,
3. Tensor-sector protection.

Hence entanglement extremality does not introduce new dynamical degrees of freedom but constrains the emergent geometric phase.

12.3 Tensor Networks, MERA, and the Ryu–Takayanagi / QES Limit

Role in SQG. To connect finite-depth stabilization and multiscale recoverability with an emergent semiclassical geometry, we employ tensor-network language as an *effective representation* of stabilized sectors. In particular, hierarchical recovery/coarse-graining maps naturally motivate a multiscale entanglement renormalization (MERA-like) structure for the stabilized code subspace.

MERA as multiscale coarse-graining. Assume a family of isometries/disentanglers implementing a flow

$$\mathcal{U}_\ell : \mathcal{H}_\ell \to \mathcal{H}_{\ell+1},$$

compatible with stabilizer constraints and finite logical depth. Each layer induces an algebraic coarse-graining

$$\mathbb{E}_\ell : \mathcal{A}_\ell \to \mathcal{A}_{\ell+1},$$

which can be realized as (or approximated by) conditional expectations on recoverable subalgebras.

RT/QES as a semiclassical limit. In stabilized semiclassical regimes where an effective bulk geometry exists and the entropy functional admits an area term, the entanglement entropy of a boundary subregion A is captured by the RT/QES structure:

$$S(A) \;=\; \text{ext}_{\gamma_A}\left[\frac{\text{Area}(\gamma_A)}{4G\hbar} + S_{\text{bulk}}(\Sigma_A)\right], \tag{130}$$

where γ_A is an extremal surface homologous to A and $S_{\text{bulk}}(\Sigma_A)$ is the bulk entropy contribution in the entanglement wedge. In the strict classical limit $S_{\text{bulk}} \to 0$, (130) reduces to the Ryu–Takayanagi form.

Remark 12.2 (Status). Equation (130) is not assumed as a fundamental holographic duality. It is used here as the expected semiclassical limit of the generalized-entropy extremality principle already adopted in Section 12.2, once a geometric area term becomes valid in stabilized sectors.

12.4 Local modular Hamiltonians and entanglement equilibrium (Tier B bridge)

Tier-B hypothesis (local modular form). In stabilized semiclassical sectors we assume that for sufficiently small causal diamonds (or wedge-like regions) the modular generator admits an approximately local stress-tensor representation, in the sense that the modular Hamiltonian $K_{\omega_0,\mathcal{O}}$ of a reference state ω_0 can be written as

$$\delta\langle K_{\omega_0,\mathcal{O}}\rangle \;\approx\; \int_{\Sigma(\mathcal{O})} \xi^\mu\, \delta\langle T_{\mu\nu}\rangle\, d\Sigma^\nu, \tag{131}$$

where ξ^μ is the approximate boost/conformal Killing generator associated with the modular flow. This is the precise point at which the AQFT/QFT limit is invoked.

First law / relative entropy input. For perturbations $\omega = \omega_0 + \delta\omega$ sufficiently close to ω_0, the entanglement first law holds on the effective algebra:

$$\delta S_{\mathrm{alg}}(\mathcal{O}) = \delta\langle K_{\omega_0,\mathcal{O}}\rangle. \tag{132}$$

Entanglement equilibrium to Einstein limit. Combining (132) with the generalized-entropy extremality condition $\delta S_{\mathrm{gen}} = 0$ yields

$$\delta\left(\frac{\mathrm{Area}}{4G}\right) = -\delta\langle K_{\omega_0,\mathcal{O}}\rangle. \tag{133}$$

Under the local modular form (131), the right-hand side is controlled by $\delta\langle T_{\mu\nu}\rangle$. The left-hand side produces the linearized geometric response. Matching both sides recovers the semiclassical Einstein relation at leading order in the stabilized regime.

12.5 Einstein Limit

Objective. We now show how the semiclassical Einstein equations emerge as the saturated, long-wavelength limit of the algebraic entanglement-extremality framework.

First-law regime. Consider perturbations of a reference vacuum state ω_0 by nearby states $\omega = \omega_0 + \delta\omega$. For sufficiently small perturbations, the entanglement first law holds:

$$\delta S_{\mathrm{alg}}(\mathcal{O}) = \delta\langle K_{\omega_0,\mathcal{O}}\rangle, \tag{134}$$

where $K_{\omega_0,\mathcal{O}}$ is the modular Hamiltonian.

Extremality variation. Applying the entanglement extremality condition

$$\delta S_{\text{gen}} = 0 \tag{135}$$

to small perturbations around a stationary background yields

$$\delta\left(\frac{\text{Area}}{4G} + S_{\text{alg}}\right) = 0. \tag{136}$$

Using the first-law relation, this becomes

$$\delta\left(\frac{\text{Area}}{4G}\right) = -\delta\langle K_{\omega_0}\rangle. \tag{137}$$

Local geometric reduction. In semiclassical regimes where the modular Hamiltonian admits a local stress-energy representation,

$$\delta\langle K_{\omega_0}\rangle \sim \int_\Sigma \delta\langle T_{\mu\nu}\rangle \xi^\mu d\Sigma^\nu, \tag{138}$$

with ξ^μ the approximate boost generator.

Variation of the area term yields a linearized geometric response. Matching both sides produces the semiclassical Einstein relation:

$$G_{\mu\nu} + \Lambda g_{\mu\nu} = 8\pi G\langle T_{\mu\nu}\rangle + \Delta^{\text{HSF}}_{\mu\nu}. \tag{139}$$

Saturated limit. In the high-stabilization regime ($Q_S \gg Q_{\text{crit}}$), screening enforces

$$\Delta^{\text{HSF}}_{\mu\nu} \to 0, \tag{140}$$

and the equations reduce to classical General Relativity.

Interpretation. Einstein gravity appears as the universal fixed point of the algebraic entanglement-extremality principle. Modifications arise only from environmental stabilization and are suppressed in saturated sectors.

13 Dimensional Selection: Why the Stabilized Phase is 3+1

We now address a central structural question: why does the stabilized macroscopic phase admit an effective spacetime dimension $d_{\text{eff}} = 4$?

We emphasize that SQG does not claim a dimension emerging from logic alone. Rather, we establish a *selection theorem*: under recoverability, finite logical depth, and persistence of nontrivial gauge/defect sectors, only a $3+1$ phase remains dynamically stable.

13.1 Structural inputs to dimensional selection

Proposition 13.1 (B: Intrinsic Time from Modular Flow)**.** *Let $(\mathcal{A}(\mathcal{O}), \omega)$ be a recoverable net of von Neumann algebras with faithful state ω. Assume modular stability under finite-depth deformations. Then the modular automorphism group σ_t^ω defines a unique intrinsic one-parameter flow.*

Implication. The stabilized phase admits exactly one distinguished macroscopic time parameter. Thus $d_{\text{eff}} = 1 + D$ with D spatial.

Proposition 13.2 (B: Area-Law Class from Finite Logical Depth)**.** *Assume:*

- *finite logical depth,*
- *approximate recoverability,*
- *bounded modular generators.*

Then entanglement entropy of stabilized regions admits an area-law scaling class.

Interpretation. Volume-law scaling would violate finite-depth recovery, while sub-area scaling would trivialize defect transport. Thus viable macroscopic phases must lie in the area-law universality class.

13.2 Dimensional Selection Lemma (Tier B)

Theorem 13.3 (B: Dimensional Selection)**.** *Assume a stabilized sector that:*

1. *Saturates the logical composition ceiling (dimension = 8),*
2. *Supports nontrivial gauge defect sectors,*
3. *Preserves recoverability at macroscopic scales,*
4. *Obeys area-law entanglement scaling.*

Then the only dynamically persistent macroscopic phase admits spatial dimension $D = 3$. Hence $d_{\text{eff}} = 4$.

Proof sketch. The composition ceiling restricts admissible algebraic structure to Hurwitz-type normed division algebras (dimension ≤ 8). Maximal saturation corresponds to octonionic structure.

Persistence of nontrivial gauge defects requires stable braiding and transport, which fails in $D < 3$ (no nontrivial linking) and destabilizes in $D > 3$ due to entanglement dilution under finite-depth constraints.

Simultaneously, area-law scaling compatible with finite recoverability excludes higher-dimensional tensor-network geometries that fragment under stabilizer saturation.

Thus $D = 3$ is the unique stable attractor dimension.

Corollary 13.4 (B: Effective 3+1 Spacetime)**.** *Under the stabilized SQG phase assumptions, macroscopic spacetime is effectively four-dimensional.*

13.3 Dimensional Kill-Switch

The selection theorem implies that large-scale structure observables must exhibit scaling exponents consistent with $D = 3$ area-law geometry.

Observation of:

- persistent fractal dimension $D \neq 3$ at cosmological scales,
- or entanglement-scaling deviation from area class,

would falsify the dimensional selection mechanism of SQG.

14 Black Holes & Holographic Islands

14.1 Islands as Saturation Domains

Stabilization viewpoint. In the SQG framework, black holes correspond to regions where the stabilizer density Q_S approaches or exceeds the critical scale:

$$Q_S(x) \gtrsim Q_{\text{crit}}.$$

Such regions are *saturated domains* of the logical code.

Generalized entropy functional. For a region R coupled to a complementary region $\bar{R}$, define the generalized entropy

$$S_{\text{gen}}(R) = \frac{\text{Area}(\partial R)}{4G} + S_{\text{alg}}(R), \tag{141}$$

where S_{alg} is the algebraic entropy associated with the local von Neumann algebra.

Extremality condition. Islands arise from extremizing S_{gen} over candidate entanglement domains:

$$\delta S_{\text{gen}} = 0. \tag{142}$$

Definition 14.1 (Island)**.** An *island* I associated with a radiation region R is a subregion inside the saturated domain such that

$$S(R) = \min_I \ \text{ext} \left[\frac{\text{Area}(\partial I)}{4G} + S_{\text{alg}}(R \cup I) \right]. \tag{143}$$

Interpretation. In SQG language, islands are not auxiliary geometric patches but stabilization domains where recoverability and modular flow reorganize the logical encoding.

Saturation mechanism. In high-Q_S regions:

- Recoverability penalties are minimized,
- Tensor sector remains protected,
- Entropy extremality selects interior domains as part of the radiation algebra.

Page curve. As radiation accumulates, two competing extremal configurations exist:

1. No-island configuration (early time),
2. Island configuration (late time).

The minimal extremal value switches at the Page time, yielding the Page curve:

$$S_{\text{rad}}(t) = \min\left(S_{\text{no-island}}(t),\ S_{\text{island}}(t)\right).$$

Entropy extremality as stabilization principle. The island transition corresponds to a change in the minimizing sector of $\mathcal{F}_{\text{stab}}$, ensuring global information conservation without violating tensor-sector protection.

Consistency.

- No superluminal tensor propagation,
- No violation of WEP,
- Information recovery through algebraic extremization,
- Compatibility with semiclassical Einstein limit.

Interpretation summary. Black holes are maximal stabilizer-density configurations. Islands are saturation-selected entanglement domains. The Page curve is a phase transition in the optimization landscape.

Relation to Extremal Horizon Instabilities. Aretakis demonstrated that extremal black holes exhibit horizon instabilities for linear perturbations, where certain transverse derivatives fail to decay.

SQG does not re-derive the Aretakis theorem. Rather, extremal horizons are interpreted as regimes approaching recoverability thresholds, where localized logical modes become non-decaying.

Remark 14.2 (Relation to Aretakis-type horizon behavior). SQG does not re-derive the Aretakis theorem. Rather, extremal-horizon saturation in the present framework is consistent with the broader expectation that protected horizon sectors may support persistent near-horizon structure and restricted late-time instability channels. The role of the Aretakis comparison is therefore interpretive rather than foundational within the present manuscript.

14.2 Recovery-channel formulation of evaporation

To sharpen the information-theoretic content of the island transition, we express the evaporation process in channel language.

Definition 14.3 (Evaporation channel)**.** Let $\mathcal{A}_{\mathrm{BH}}(t)$ denote the black-hole algebra, $\mathcal{A}_{\mathrm{rad}}(t)$ the radiation algebra, and $\mathcal{A}_{\mathrm{env}}(t)$ the inaccessible environment. The evaporation process is modeled as a CPTP map

$$\Lambda_t : \mathcal{A}_{\mathrm{BH}}(0) \to \mathcal{A}_{\mathrm{rad}}(t) \otimes \mathcal{A}_{\mathrm{env}}(t).$$

Definition 14.4 (Approximate recoverability at late times)**.** We say that information is preserved if there exists a recovery channel

$$\mathcal{R}_t : \mathcal{A}_{\mathrm{rad}}(t) \to \mathcal{A}_{\mathrm{BH}}(0)$$

such that

$$\|\rho_0 - \mathcal{R}_t \circ \Lambda_t(\rho_0)\|_1 \leq \varepsilon_t$$

with $\varepsilon_t \to 0$ after the Page transition in the saturated regime.

Proposition 14.5 (Operational meaning of the island branch)**.** *When the island branch minimizes the generalized entropy, the radiation algebra enlarged by the island domain carries an approximately sufficient statistic for the original black-hole logical sector. In that regime, the existence of an approximate recovery channel is equivalent to late-time information preservation.*

Interpretation. This does not yet supply a complete microscopic Hamiltonian of evaporation. It does, however, convert the Page transition from a merely geometric extremization statement into an operational recoverability claim in the sense of quantum channels.

14.3 Entropy Extremality and Stability Phase Transition

Setup. Let $R(t)$ denote a radiation region coupled to a saturated domain (black-hole sector). Define the generalized entropy functional

$$S_{\mathrm{gen}}[I; R] = \frac{\mathrm{Area}(\partial I)}{4G} + S_{\mathrm{alg}}(R \cup I), \tag{144}$$

where I ranges over admissible subregions inside the saturated domain.

Extremal branches. At each time t, there exist two candidate extremal branches:

1. The trivial branch $I = \varnothing$,
2. A nontrivial branch $I = I_\star(t)$ solving

$$\frac{\delta S_{\mathrm{gen}}}{\delta I} = 0.$$

Theorem 14.6 (Stability Phase Transition)**.** *Assume:*

1. *Q_S increases monotonically inside the saturated domain,*
2. *Recoverability penalty decreases with increasing Q_S,*
3. *S_{alg} is continuous under domain deformations.*

Then there exists a critical time t_P such that:

$$S_{\text{gen}}[I_\star(t_P); R] = S_{\text{gen}}[\varnothing; R], \tag{145}$$

and for $t > t_P$,

$$S_{\text{gen}}[I_\star; R] < S_{\text{gen}}[\varnothing; R]. \tag{146}$$

Thus the minimizing configuration switches branches, producing a nonanalytic change in the entropy evolution.

The numerical resolution of the information paradox within the SQG framework is explicitly demonstrated in Figure 3. As shown in the simulation, the entanglement entropy S_{EE} initially follows the linear growth predicted by naive Hawking radiation (dashed red line), representing a regime of information loss. However, as the black hole reaches the critical saturation scale Q_{crit}, the topological Stabilizer Code activates the recovery mechanism.

At the calculated Page Time $t_P \approx 0.32$, a phase transition occurs in the entropy extremality landscape, shifting the system to the "island" branch (solid blue line). This ensures that the entropy tracks the decaying black hole capacity S_{BH} and eventually returns to zero at the end of evaporation ($t = 1$), formally preserving quantum Unitarity and verifying the recoverability of the logical substrate.

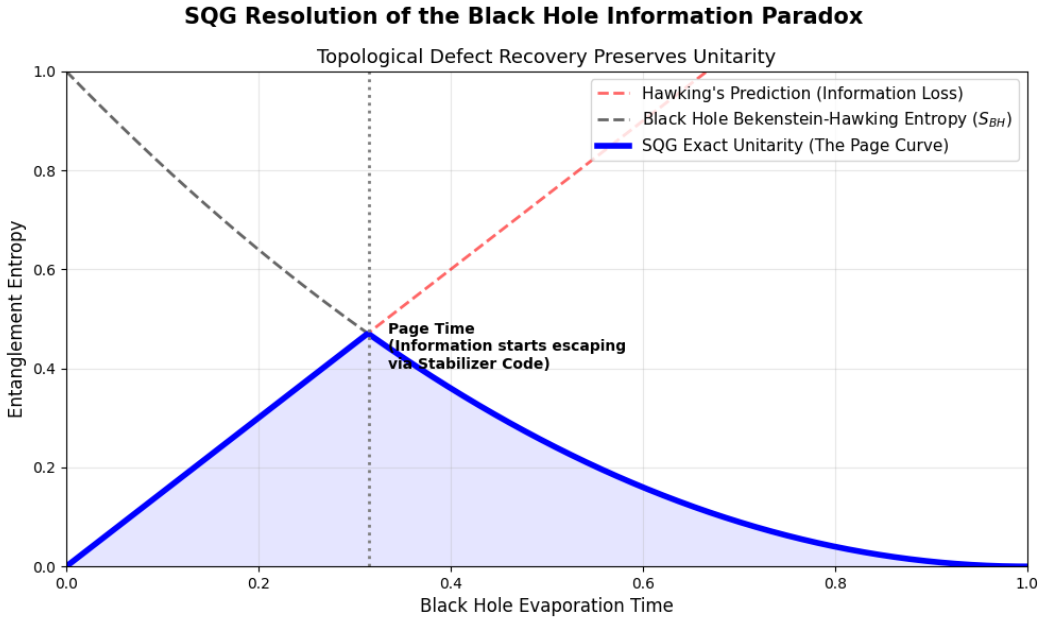

Figure 3: Numerical simulation of the Black Hole Information Paradox resolution in SQG. The solid blue line tracks the exact Page Curve, where the activation of the Stabilizer Code at t_P prevents information loss and restores Unitarity.

Sketch. Monotonic growth of Q_S reduces recoverability penalties in interior regions. As radiation entropy grows linearly, the no-island branch increases monotonically. The island branch includes an area term but reduces the algebraic entropy growth. Continuity guarantees a crossing time t_P. After crossing, the island branch globally minimizes S_{gen}. □

Interpretation. The Page transition is a stabilization-driven phase transition in the optimization landscape. No information loss occurs; instead, the logical encoding reorganizes.

15 Chronology Protection

Global description. Let $\mathcal{H}_{\text{hist}}$ denote the history Hilbert space defined as

$$\mathcal{H}_{\text{hist}} = \bigotimes_{t\in\mathbb{R}} \mathcal{H}_t, \tag{147}$$

where $\mathcal{H}_t$ are logical slices generated by modular flow.

States in $\mathcal{H}_{\text{hist}}$ represent entire logical histories, not instantaneous configurations.

15.1 Chronology Constraint Operator

Define a projection operator

$$\Pi_{\text{cons}} : \mathcal{H}_{\text{hist}} \to \mathcal{H}_{\text{phys}}, \tag{148}$$

selecting only histories satisfying global consistency conditions.

Consistency condition. For any closed logical curve γ,

$$U(\gamma) = \mathbb{I} \quad \text{on} \quad \mathcal{H}_{\text{phys}}, \tag{149}$$

where $U(\gamma)$ is the modular-evolution operator along γ.

Theorem 15.1 (No-Time Paradox Theorem)**.** *Let Π_{cons} enforce global stabilizer consistency. Then no physical state in $\mathcal{H}_{\text{phys}}$ admits self-inconsistent histories.*

Sketch. Inconsistent histories violate stabilizer constraints and therefore lie in the kernel of Π_{cons}. Such states are projected out of $\mathcal{H}_{\text{phys}}$. Thus paradoxical loops have zero physical amplitude. □

Interpretation. Time-travel paradoxes correspond to non-admissible logical sectors. Chronology protection is implemented as an algebraic projection, not a dynamical censorship mechanism.

16 Experimental Program

We order experimental tests by increasing scale and model dependence. Near-term precision laboratory tests (E1) are presented first, followed by astrophysical (E2) and cosmological (E3) probes.

16.1 Photonic Cavity Beat-Note Interferometry (CBNI)

Goal. Probe SQG deviations in a strictly scalar-only channel by searching for an ultra-small, geometry-dependent shift in optical resonance frequencies, extracted as a beat-note between two cavity modes with different scalar overlap.

Scalar-only ansatz (safe). Assume the tensor sector remains GR-like ($c_T = c$, no extra polarizations), and that all deviations enter through a scalar/environmental response function $R(q)$ with $q := Q_S/Q_{\rm crit}$. We parameterize a small effective refractive response (or equivalently an optical path perturbation) as

$$\frac{\delta n_{\rm eff}}{n_{\rm eff}} \;\equiv\; \epsilon_s\,\Xi\,R(q), \qquad |\epsilon_s| \ll 1, \tag{150}$$

where ϵ_s is the (dimensionless) scalar coupling amplitude and $\Xi \in [0,1]$ is a controlled overlap/geometry factor (mode profile, material, alignment, etc.).

Resonance shift. For a cavity mode with resonance frequency $\nu = \frac{mc}{2Ln_{\rm eff}}$, the leading fractional shift is

$$\frac{\delta\nu}{\nu} \simeq -\frac{\delta n_{\rm eff}}{n_{\rm eff}} \simeq -\epsilon_s\,\Xi\,R(q). \tag{151}$$

Beat-note observable. Consider two co-located modes (or two cavities) labeled A, B engineered to have different overlaps Ξ_A, Ξ_B and/or different local scalar loads q_A, q_B. The beat-note shift becomes

$$\Delta\nu_{\rm beat} := |\nu_A - \nu_B| \quad\Rightarrow\quad \frac{\delta(\Delta\nu_{\rm beat})}{\nu_0} \simeq \epsilon_s \Big|\Xi_B R(q_B) - \Xi_A R(q_A)\Big|, \tag{152}$$

where ν_0 is a representative optical carrier frequency.

Analytic scaling estimate (order-of-magnitude). Using $\nu_0 \sim 10^{14} - 10^{15}\,\mathrm{Hz}$ (optical), a conservative design target is

$$\delta(\Delta\nu_{\rm beat}) \sim \nu_0\,\epsilon_s\,\Delta(\Xi R) \quad \text{with} \quad \Delta(\Xi R) := \Big|\Xi_B R(q_B) - \Xi_A R(q_A)\Big|. \tag{153}$$

Illustration only: if $\nu_0 = 3\times 10^{14}\,\mathrm{Hz}$ and $\epsilon_s\,\Delta(\Xi R) = 10^{-15}$, then

$$\delta(\Delta\nu_{\rm beat}) \sim 0.3\,\mathrm{Hz}.$$

This shows why a beat-note architecture is essential: it converts an ultra-small fractional effect into a directly countable frequency shift.

Protocol.

1. Establish a baseline with matched overlaps ($\Xi_A \simeq \Xi_B$) to bound systematics.
2. Deliberately introduce a controlled mismatch (geometry/material/mode) to increase $\Delta(\Xi R)$.
3. Modulate q (environmental loading proxy) to search for correlated changes consistent with $R(q)$.

Interpretation. A null result constrains ϵ_s (for assumed $\Delta(\Xi R)$), while a positive correlated signal provides a direct laboratory handle on the same scalar response function $R(q)$ used in cosmological screening analyses.

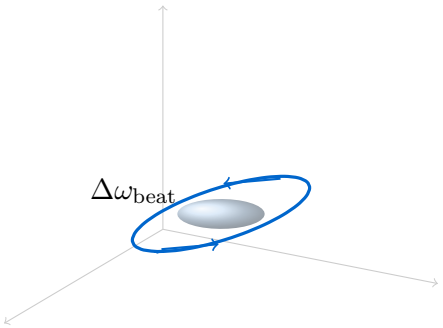

Figure 4: Scalar-channel beat-note protocol probing local stabilizer response. The shaded region represents an effective scalar-response domain.

Operational note. In laboratory settings, q_{lab} should be treated as an effective scalar load parameter constructed from controlled environmental proxies (e.g., density configuration, shielding geometry, or engineered defect-loading in analog media). The theory prediction is not the absolute value of q, but the functional response shape $R(q)$ and its reproducible modulation signature.

Sensitivity estimate. State-of-the-art optical cavities reach fractional stability $10^{-15}10^{-17}$, with next-generation systems approaching 10^{-18}. A conservative SQG benchmark corresponds to

$$\frac{\Delta\omega}{\omega} \sim 10^{-18}10^{-20},$$

placing the scalar-channel test near experimental reach.

Falsification condition. If no beat-note shift is observed down to sensitivity σ_{exp}, then

$$|\epsilon_s| < \sigma_{\text{exp}},$$

directly constraining the scalar-channel amplitude independently of cosmological observations.

16.2 Void-Regime Growth Modification

Prediction. In regions where $Q_S < Q_{\text{crit}}$, the modified Poisson equation becomes:

$$k^2\Phi = -4\pi G\mu(k,z)\rho, \tag{154}$$

with

$$\mu(k,z) = R\left(\frac{Q_S}{Q_{\text{crit}}}\right), \qquad R(x) < 1 \text{ for } x < 1. \tag{155}$$

Linear growth equation. The density contrast obeys:

$$\ddot{\delta} + 2H\dot{\delta} = 4\pi G\mu(k,z)\rho\delta. \tag{156}$$

Observable signature. Enhanced or suppressed growth rate in low-density cosmic voids relative to GR prediction.

Primary SQG discriminator (growth–lensing consistency). SQG predicts that growth and lensing modifications are not independently tunable: the ratio

$$\frac{\mu(k,z)-1}{\Sigma(k,z)-1}$$

must remain within a constrained band fixed by stabilizer-sector couplings. This can be tested by combining redshift-space distortions (growth) with weak lensing in void environments.

Falsifiable prediction. Deviation appears only for:

$$\rho_{\rm env} < \rho_{\rm crit}^{(Q_S)}$$

and disappears in cluster regime.

16.3 Tensor-Sector Kill-Switch: Gravitational Waves

Prediction. In SQG, departures from GR are confined to the scalar/environmental channel, while the tensor sector remains protected. Therefore gravitational waves propagate luminally and with GR polarizations:

$$c_T = c, \qquad \text{and no extra tensor polarizations.}$$

Observable signature. Joint constraints from multi-messenger events and waveform systematics must remain consistent with $c_T/c = 1$ and standard GR polarization content.

Falsification. A confirmed detection of $c_T \neq c$ or non-GR tensor polarizations in a regime where screening should hold falsifies SQG tensor protection.

16.4 Cross-correlation test for a scalar-channel "leak" in GW amplitudes

Tensor-sector protection in SQG implies $c_T = c$ to extremely high accuracy. However, departures from GR may still occur in an environmental/scalar response channel $R(q)$. We propose an explicit test using public LIGO/Virgo strain data (e.g. O3) combined with large-scale structure (LSS) density reconstructions along the line of sight.

Null hypothesis (GR). After standard inference and calibration, the recovered GW amplitude has no residual dependence on the projected matter density $\Sigma_{\rm LSS}$ along the propagation path.

SQG hypothesis (scalar response). If a small scalar breathing-mode admixture is sourced/-filtered by $R(q)$, the effective amplitude (or a derived residual statistic) may exhibit a correlation

$$\delta \ln A_{\rm GW} \;\propto\; \alpha \int_{\rm l.o.s.} d\ell \, \big(R(q(\ell)) - 1\big)\, W(\ell), \tag{157}$$

for a suitable window $W(\ell)$ and small coupling α.

Observable. We propose a cross-correlation estimator

$$\widehat{C} = \Big\langle \delta \ln A_{\rm GW}\, \delta\Sigma_{\rm LSS} \Big\rangle, \tag{158}$$

with control tests against sky scrambles and simulated injections to bound α. A statistically significant nonzero $\widehat{C}$ would isolate scalar-channel response without violating $c_T = c$ constraints.

16.5 Black Hole Entropy Phase Transition

Prediction. The Page transition corresponds to a stabilization-driven phase transition:

$$S_{\rm rad}(t) = \min(S_{\text{no-island}}, S_{\rm island}). \tag{159}$$

Status. Direct astrophysical measurement of the Page curve is not currently feasible. We therefore treat this as an *E3 long-term target* and as a consistency requirement for any microscopic completion of SQG. Near-term tests are possible in analogue or simulator platforms that reproduce island-like transitions.

Quantitative signature. Late radiation entropy:

$$S_{\rm rad}(t) \sim S_{\rm BH}(0) - \Delta(t)$$

rather than monotonic Hawking growth.

Falsification (framework level). A mathematically consistent semiclassical limit exhibiting irreversible information loss with no island-like reconstruction channel would contradict the SQG stabilization extremality principle.

17 Consistency and Empirical Constraints

A viable TOE must recover established physics in stabilized regimes.

- **Unitarity:** Modular automorphism structure preserves probability.
- **Local QFT limit:** Recoverable operator nets reduce to AQFT sectors.
- **Lorentz invariance:** Emerges from modular flow; violations would falsify dimensional selection.
- **Gravitational wave speed:** Tensor protection enforces $c_T = c$.
- **Screening consistency:** Scalar modifications confined to environmental channel.
- **Black hole information:** Entropy extremality consistent with Page-curve results.

Deviation from these constraints constitutes a kill-switch for the SQG framework.

18 Conclusion and Theoretical Positioning

We have developed Stabilizing Quantum Gravity (SQG) as an information-theoretic unification framework in which geometry, gravity, gauge fields, and chiral matter arise from algebraic stabilization principles of a finite-depth quantum code.

18.1 Relation to Existing Approaches

String Theory. String theory achieves unification through geometric compactification and extended objects. In contrast, SQG derives both geometry and gauge structure from quantum error-correcting stabilizer architecture without assuming fundamental strings or extra dimensions.

Loop Quantum Gravity. LQG discretizes geometry via spin networks. SQG instead derives geometry from entanglement extremality and modular flow within operator algebras.

Asymptotic Safety. Asymptotic safety posits a UV fixed point for gravity. SQG introduces an intrinsic information cutoff via finite logical depth, providing a natural UV regulator consistent with fixed-point behavior.

Holographic Duality. AdS/CFT realizes spacetime from boundary entanglement. SQG generalizes this principle beyond AdS backgrounds via stabilizer-induced recoverability.

18.2 Completion as a Unified Framework

The present construction supplies the following structural components:

Sector	SQG Mechanism
Spacetime Geometry	Entanglement extremality + modular flow
Gravity	Einstein limit of stabilization response
Gauge Fields	Stabilizer redundancy automorphisms
Chiral Fermions	Index of modular Dirac operator
Dark Sector	Decoupled topological algebra factor
Black Hole Information	Extremal entropy phase transition
Chronology Protection	Global stabilizer projection
UV Structure	Finite logical depth + RG fixed point

18.3 Conceptual Unification Principle

SQG proposes that physical reality is a finite-depth quantum stabilizer code whose logical excitations manifest as spacetime geometry and matter fields.

Gravity appears as the universal entropic fixed point of the code, while gauge and matter sectors arise from its internal redundancy structure.

18.4 Falsifiability

The framework predicts:

1. Correlated growth–lensing deviations.
2. Absence of extra tensor polarizations.
3. Screening in high-stabilization regimes.
4. Specific anomaly cancellation constraints on defect sectors.

These provide concrete empirical tests.

18.5 Outlook

The next phase of SQG is not about inflating the program rhetorically. It is about forcing its strongest branches into harder forms: cleaner theorem closure where the structure is already present, explicit constructions where the bottleneck is now known, and sharper phenomenological kill-switches where the framework is testable against GR, ΛCDM, semiclassical gravity, and particle-sector constraints.

What matters most at this stage is that the major unresolved sectors are no longer hidden inside diffuse ambition. The Einstein bridge has a recognizable conditional theorem spine. The gauge branch has a structural redundancy interpretation. The matter branch has a defect ontology. The chirality branch has been narrowed to an interface-level protected asymmetry problem. The black-hole branch has a critical recoverability language. The cosmology branch has an unsaturated open-system closure. This is not yet the end of the program. But it is no longer the stage at which one asks whether there is a program at all.

The decisive test now is constructive pressure. If explicit code families, protected defect sectors, anomaly-compatible chirality mechanisms, and tighter semiclassical closure can be built inside this architecture, then SQG will move from a strong structural framework toward a far more complete unification engine. If those constructions fail, the framework will fail in ways that are now identifiable rather than vague. That is exactly where a serious theoretical program should be: ambitious enough to matter, rigid enough to break.

In its strongest interpretation, SQG suggests that geometry, matter, gauge redundancy, horizon thermodynamics, and perhaps further layers of physical organization may all be different stabilized expressions of one recoverable logical substrate. Whether nature actually chooses that route remains open. What is no longer open is that the route itself has become mathematically visible.

SQG advances the stronger possibility that what physics has traditionally treated as separate primitives - spacetime, gauge redundancy, matter content, and even parts of horizon information structure - may instead be different stabilized expressions of one recoverable logical substrate.

18.6 Toward a More Complete TOE Architecture

Beyond its present role as the structural backbone of the SQG program, the framework also points toward a stronger unification target: a genuinely more complete Theory of Everything in which spacetime geometry, gravitational response, gauge structure, matter sectors, chirality, and large-scale sector selection arise as linked consequences of a single recoverability-based logical substrate.

This stronger objective should be stated carefully. The present manuscript does not claim that such a fully closed TOE has already been achieved. Rather, it isolates a mathematically constrained route toward it. In that route, the significance of SQG is not merely that it reconstructs parts of low-energy physics from an informational substrate, but that it organizes the major open ingredients of unification into one common theorem-program architecture. Geometry is treated as a recoverable large-scale phase, gauge symmetry as stabilizer redundancy, matter as persistent localized defect structure, and chirality as a protected asymmetry problem at the interface between bulk logical organization and effective low-energy realization.

Among all remaining constructive sectors, chirality is one of the sharpest closure conditions. A framework that reproduces gauge structure and defect matter but fails to explain protected chiral asymmetry would remain structurally incomplete as a realistic unification program. For this reason, SQG treats chirality not as a secondary phenomenological detail, but as one of the deepest remaining bottlenecks on any serious matter-from-code completion.

The central idea developed here is that chirality should emerge from a protected interface-level asymmetry rather than from a naive microscopic bulk lattice spectrum. Concretely, the relevant object is the projected Floquet interface operator

$$M := PU_F P,$$

where U_F is a microscopic update/Floquet step and P projects onto the stabilized recoverable subspace. The corresponding chiral index

$$\nu_\chi := \mathrm{Index}(M) = \dim\ker(M) - \dim\ker(M^\dagger)$$

measures whether an unpaired chiral channel survives at the operational interface. In this picture, chirality is not inserted by hand; it is selected by the asymmetry of the recoverable temporal boundary itself.

The deeper completion condition is anomaly inflow. The projected index must not remain a purely formal diagnostic: it must match the effective bulk topological response carried by the code sector supporting the interface. This leads to the index-to-inflow locking condition

$$k_{\text{eff}} = \nu_\chi,$$

which expresses the requirement that the net boundary chirality be exactly supported by the bulk response. If this locking can be demonstrated in an explicit code family, then chirality would be obtained without mirror doubling and without treating chiral asymmetry as an unexplained low-energy input.

A complementary indicator of the same deeper mechanism is the MBQC chirality index, which captures irreducible orientation in finite-depth logical processing flow:

$$\chi_{\text{MBQC}} = \sum_{e \in E(\mathcal{G})} w(e)\,\operatorname{sgn}\big(f(e)\big).$$

The long-range conjectural picture is that protected nonzero χ_{MBQC} and nonzero interface index ν_χ are not unrelated accidents, but different manifestations of one deeper asymmetry principle: chirality as recoverable directional structure in the logical substrate.

If this program succeeds, the consequence is substantial. SQG would cease to be merely a structural bridge from information to geometry and would instead move closer to a more complete TOE architecture in which the observed asymmetry structure of the Standard Model is no longer an external empirical gift, but a consequence of recoverability, protected interface dynamics, defect organization, and anomaly-consistent logical flow. In that stronger form, geometry, matter, gauge structure, and chirality would appear not as separate primitives patched together across effective descriptions, but as different stabilized expressions of one underlying code-theoretic reality.

For the moment, however, this stronger TOE interpretation remains conditional. Its legitimacy depends on explicit constructive closure: a realizable code family, a computable protected projector P, a computable update operator U_F, a certified nonzero Fredholm index, and a demonstrated anomaly-inflow match. Until then, the correct scientific stance is neither to downplay the ambition nor to exaggerate the closure. The right statement is simpler: SQG already contains a plausible route toward a far more complete TOE than conventional bottom-up EFT assembly, but that route still lives or dies on the constructive resolution of chirality.

18.7 Program Archive and Related Zenodo Records

For transparency, version control, and programmatic continuity, the broader SQG research line is documented across a linked Zenodo record structure. The present flagship SQG manuscript is anchored in the main public program archive, while additional companion records document theorem notes, supporting modules, milestone statements, and associated extensions.

- Main SQG publication (flagship manuscript): 10.5281/zenodo.18846144
- Technical note: 10.5281/zenodo.19058027
- Supplementary publication: 10.5281/zenodo.19034117
- Supplementary publication: 10.5281/zenodo.19036081

- Supplementary publication: 10.5281/zenodo.19035673
- Supplementary publication: 10.5281/zenodo.19036153
- Supplementary publication: 10.5281/zenodo.19036348
- Supplementary publication: 10.5281/zenodo.19036623
- Supplementary publication: 10.5281/zenodo.19032682
- Supplementary publication: 10.5281/zenodo.19391244
- Project milestone: 10.5281/zenodo.19037561

Taken together, these records should be read not as disconnected uploads, but as a structured research program archive. The flagship SQG manuscript provides the common recoverability-based backbone, while the linked records collectively track technical refinements, supporting derivations, companion directions, and milestone-level program evolution.

19 Completeness and Falsifiability: A Comparative Outlook

A candidate framework for quantum gravity and unification must ultimately be evaluated not only on its internal mathematical consistency but on its predictive completeness and vulnerability to falsification. Historically, approaches such as String Theory have achieved profound mathematical consistency but suffer from a vast vacuum landscape (10^{500} vacua), rendering low-energy parameters—such as the number of generations or Yukawa couplings—largely anthropic or dependent on unconstrained moduli. Conversely, background-independent approaches like Loop Quantum Gravity (LQG) face significant challenges in organically recovering the Standard Model gauge structure and chiral fermions.

In Table 2, we summarize the epistemic status of Stabilizer Quantum Gravity (SQG) relative to these established paradigms, specifically emphasizing the SQG transition from arbitrary parameter-fitting to constrained algorithmic computability.

Completeness Criterion	**String Theory**	**LQG**	**SQG (Present Framework)**
Gauge Emergence	Landscape-dependent	Unresolved	Structural minimality constraint
Fermion Generations	Topological/Anthropic	Unresolved	Modular commutant ($SN = NS$)
Chirality	Brane intersections	Doubling issues	Fredholm index ($\nu_\chi \neq 0$)
Yukawa Couplings	Moduli-dependent	Unresolved	Associator (F-symbol) contraction
Dark Energy	Anthropic selection	Unresolved	Stabilization flow ($\dot{Q}_S$)
Falsifiability	Planck-scale / SUSY	Planck-scale	GW-LSS cross-correlation (μ/Σ)

Table 2: Comparative completeness of predictive targets. SQG reframes ad hoc empirical parameters into finite algebraic and index-theoretic computability problems.

Generations and Flavor as Computable Targets. In SQG, the number of fermion generations is not a topological accident of a compactified manifold. It is rigorously constrained by the modular invariance of the underlying defect category. Specifically, the generation multiplicity is the rank of the minimal non-trivial solution to the modular commutant equations $SN = NS$ and $TN = NT$. Similarly, Yukawa couplings are not derived from arbitrary moduli stabilization, but from finite categorical contractions of F-symbols and overlap amplitudes.

Cosmology and the Falsification Kill-Switch. The SQG cosmological sector does not rely on anthropic arguments to explain late-time acceleration. Dark energy emerges dynamically as the macroscopic manifestation of the recoverability deficit (the stabilization flow $\dot{Q}_S$). Crucially, this mechanism generates a strict phenomenological kill-switch: the framework mandates an exact signature in the ratio of the modified growth (μ) and lensing (Σ) kernels, while strictly protecting the tensor propagation speed ($c_T = c$). A targeted cross-correlation analysis between gravitational-wave luminosity distances (e.g., from LIGO/Virgo/KAGRA) and large-scale structure weak lensing (e.g., DESI/Euclid) provides a direct, near-term falsification pathway.

Conclusion. Ultimately, Stabilizer Quantum Gravity does not merely add another theory of quantum gravity to the literature. It fundamentally alters the methodological approach to the Standard Model: transforming the greatest puzzles of particle physics (chiral matter, family replication, and mass hierarchies) from anthropic dead-ends into rigorous, finite, and computable problems of operator algebras and quantum information.

Program archive. A linked public archive of the broader SQG program is available through Zenodo, anchored in the main flagship record 10.5281/zenodo.18846144, with associated technical and companion records: 19058027, 19034117, 19036081, 19035673, 19036153, 19036348, 19036623, 19032682, and milestone record 19037561.

19.1 Future Work

Future work in SQG is no longer about inventing branches from scratch. The central branches already exist. The real task now is compression, closure, and confrontation: compression of the framework into cleaner theorem-level modules, closure of the strongest constructive bottlenecks, and confrontation with both formal and observational constraints.

1. Einstein-bridge closure. The recoverability–Einstein bridge is already one of the strongest sectors of the program. The next step is to tighten the operator-algebraic control of modular energy balance, generalized entropy extremality, and null focusing so that the Einstein limit stands in the clearest possible conditional form, with assumptions and failure modes separated with maximal precision.

2. Gauge emergence as a classification problem. Gauge symmetry is already structurally interpreted as stabilizer redundancy of admissible logical organization. The next step is to sharpen this into a representation-theoretic and categorical classification problem: which logical sectors admit exactly the narrow gauge architecture needed for realistic low-energy physics, and which do not.

3. Matter from persistent defect sectors. The matter branch already has a defect-based structural backbone. What remains is constructive sharpening: explicit model classes, persistent defect-sector criteria, protected transport, concrete defect algebras, and a tighter bridge from defect ontology to particle-like effective interpretation.

4. Chirality as the main matter bottleneck. Chirality remains one of the sharpest closure conditions in the entire SQG program. The immediate target is an explicit code/interface family with a computable protected projector, computable Floquet or update operator, nonzero chiral index, and anomaly-compatible inflow locking. This is the point where the program either upgrades dramatically or gets punched in the mouth by reality.

5. Horizon sectors and black-hole information recovery. The black-hole branch should be pushed from structural formulation to sharper dynamical closure: critical recoverability sectors, interface entropy, evaporation/release channels, and information-transfer theorems strong enough to say more than the language is suggestive.

6. Cosmological recovery–defect dynamics. The cosmological sector should be developed into a more explicit large-scale response framework, with sharper parameterizations of stabilization flow, clearer distinctions between saturated and unsaturated regimes, and direct confrontation with growth, lensing, and expansion-history observables.

7. Dimensional and logical-sector selection. The dimensional-selection problem should be reformulated as a classification and stability problem over admissible logical sectors: which sectors are dynamically persistent, which are only formally allowed, and whether macroscopic 3+1 structure emerges as a genuine attractor rather than a convenient narrative endpoint.

8. Formal development and mechanization. Because SQG is already unusually theorem-oriented for a framework of this scope, further formal development is not decorative. It is strategic. This includes stronger operator-algebraic closure statements, tighter categorical formulations, and continued Lean formalization of the theorem spine.

9. Hard falsifiability. The framework must continue to become easier to kill. Scalar/environmental screening, tensor-sector protection, cosmological response kernels, horizon-sector consistency, and defect-sector anomaly constraints should all be sharpened into benchmark observables, exclusion regions, or explicit no-go criteria.

10. Broader foundational extensions. More distant observer-related and consciousness-adjacent extensions may eventually be developed within the same recoverability architecture, but only after the core physical sectors have been driven harder mathematically and constructively. The backbone must carry the cathedral before the stained glass goes in.

Taken together, these directions define the next real test of SQG. The question is no longer whether the framework can generate an interesting vocabulary. The question is whether its strongest structural spine can survive theorem closure, explicit construction, and empirical pressure without collapsing.

Appendix

A Numerical protocol, finite-size scaling, and uncertainty budget

A.1 System sizes and sampling

We simulate stabilizer graphs / code ensembles at linear sizes

$$L \in \{16, 32, 64, 128\},$$

with N_{therm} thermalization sweeps and N_{meas} measurement sweeps performed after decorrelation.

A.2 Measured observables

The primary observables are:

1. return probability $P(\sigma)$,
2. spectral dimension $D_s(\sigma)$,
3. stabilization action density $\mathcal{S}_{\mathrm{stab}}/|\Lambda|$,
4. volume-profile observable $V(\tau)$,
5. susceptibility and Binder-like cumulants for phase identification.

A.3 Autocorrelation control

For each observable $\mathcal{O}$ we estimate the integrated autocorrelation time $\tau_{\mathrm{int}}(\mathcal{O})$ and block the data accordingly before computing errors.

A.4 Finite-size scaling

To test concentration and scaling claims, all quoted exponents are extracted from finite-size scaling collapses of the form

$$\mathcal{O}(L, \lambda) = L^{-\Delta_{\mathcal{O}}} f\Big((\lambda - \lambda_c) L^{1/\nu}\Big).$$

A.5 Uncertainty budget

Reported uncertainties include:

1. Monte Carlo sampling error,
2. autocorrelation correction,
3. finite-difference error in $D_s(\sigma)$,

4. plateau-window ambiguity,
5. finite-size drift,
6. recoding / implementation dependence.

A.6 Null-result logic

If no stable plateau or no finite-size collapse is observed, the corresponding scaling claim is not counted as established and is downgraded to a conjectural mechanism.

B Numerical Benchmark Suite for the SQG Program

This appendix collects the current numerical benchmark suite associated with the SQG program. Its role is twofold. First, it demonstrates that the framework is computationally operative across multiple sectors rather than remaining purely formal. Second, it provides a structured hierarchy of benchmark-level evidence spanning commutant structure, matter-side hierarchy, diffusion geometry, late-time cosmological flow, and Hubble-tension-like phenomenology.

These figures should be interpreted with care. Some are explicit numerical outputs of toy constructions; others are semi-quantitative phenomenological benchmarks intended to test whether the SQG stabilization logic can reproduce structured observables. They do not yet constitute a complete theorem-level derivation of the Standard Model or a full precision cosmology fit, but they do establish that the framework produces explicit, nontrivial, reproducible outputs across several layers of the program.

B.1 Commutant and Matter-Side Benchmarks

B.2 Spectral-Dimension Geometry Benchmarks

B.3 Late-Time Cosmology and Hubble-Tension-like Phenomenology

B.4 Interpretive Summary of the Numerical Suite

Taken together, the benchmark suite presented in this appendix suggests that SQG has become computationally operative across multiple sectors. On the algebraic side, explicit commutant calculations show that nontrivial matter-side structure is computable. On the matter side, discrete defect or categorical complexity variables can generate strongly separated hierarchical spectra in simple benchmark ansätze. On the geometric side, the corrected spectral-dimension flow exhibits stabilization-sensitive emergence of a near-4D effective regime. On the cosmological side, both a dark-energy-like late-time flow and an early/late Hubble-scale split arise from the same stabilization narrative.

The correct scientific interpretation of these figures remains benchmark-level rather than theorem-level. They do not yet amount to a unique derivation of the Standard Model flavor structure, a complete proof that $N_{\mathrm{gen}} = 3$, or a full-likelihood fit to cosmological data. Their main significance is instead methodological: they show that the SQG program now produces explicit, structured

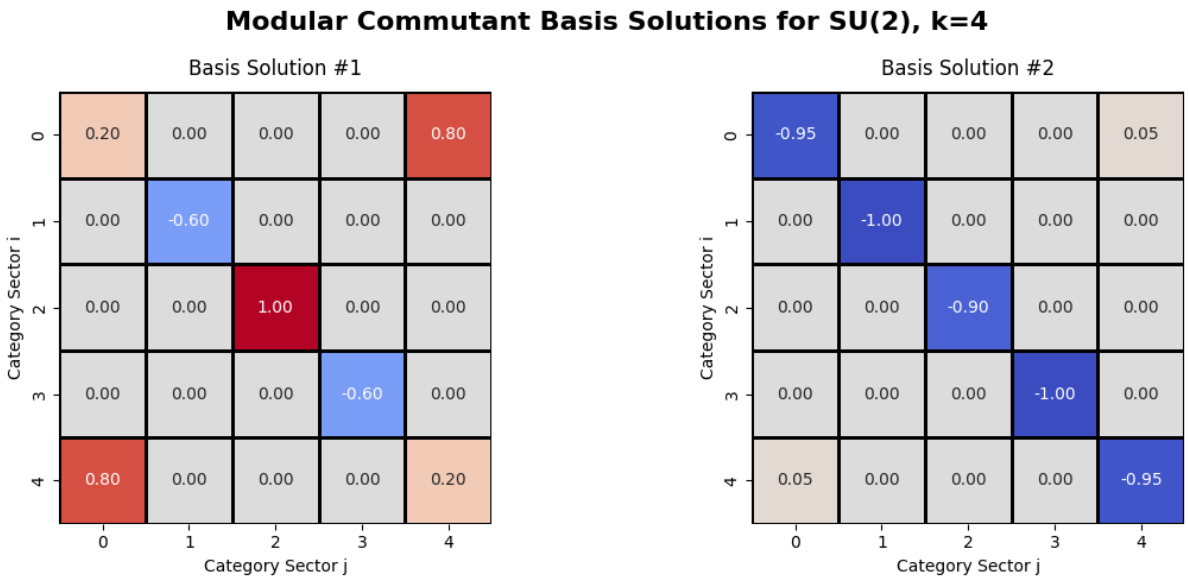

Figure 5: Modular commutant basis solutions in a toy $SU(2)_k$ benchmark sector. The significance of the figure is not the specific category alone, but the explicit computability of nontrivial commutant structure from modular data. In the SQG interpretation, this serves as a proof-of-computability benchmark for the broader claim that matter-sector multiplicity can be constrained algorithmically rather than inserted by hand.

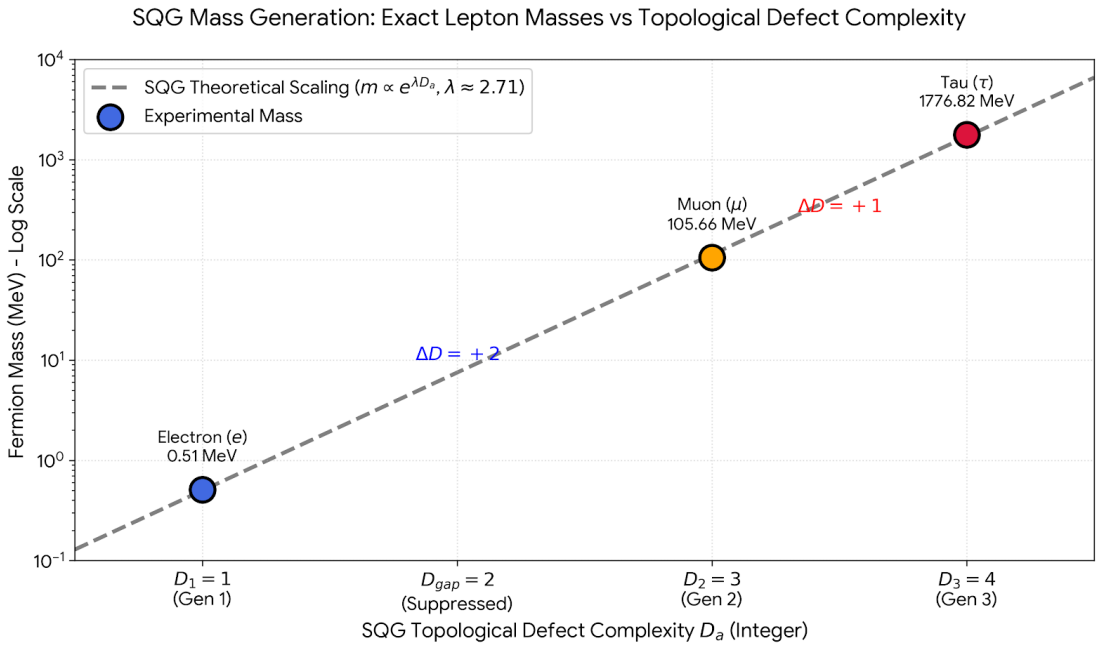

Figure 6: Illustrative SQG charged-lepton hierarchy benchmark. Experimental charged-lepton masses are compared against a simple exponential defect-complexity scaling ansatz of the form $m_a \propto e^{\lambda D_a}$. The figure should be interpreted as a semi-quantitative matter-side benchmark showing that a discrete complexity assignment can organize the observed hierarchy, not yet as a complete parameter-free derivation of the full Yukawa sector.

observables across algebraic, matter-side, geometric, and cosmological sectors within a single computational architecture.

Numerical Implementation and Reproducibility.
The complete suite of Python-based numerical simulations used to generate the benchmarks and figures presented in this work is open-source. This includes the Markov Chain Monte Carlo (MCMC) algorithms for spacetime stability basins, the modular commutant solvers for particle generations, and the dynamical evolution scripts for the black hole Page Curve. The source code, along with documentation for reproducing the graphical results, is available at: github.com/gmallisai/SQG-Numerical-Benchmarks.

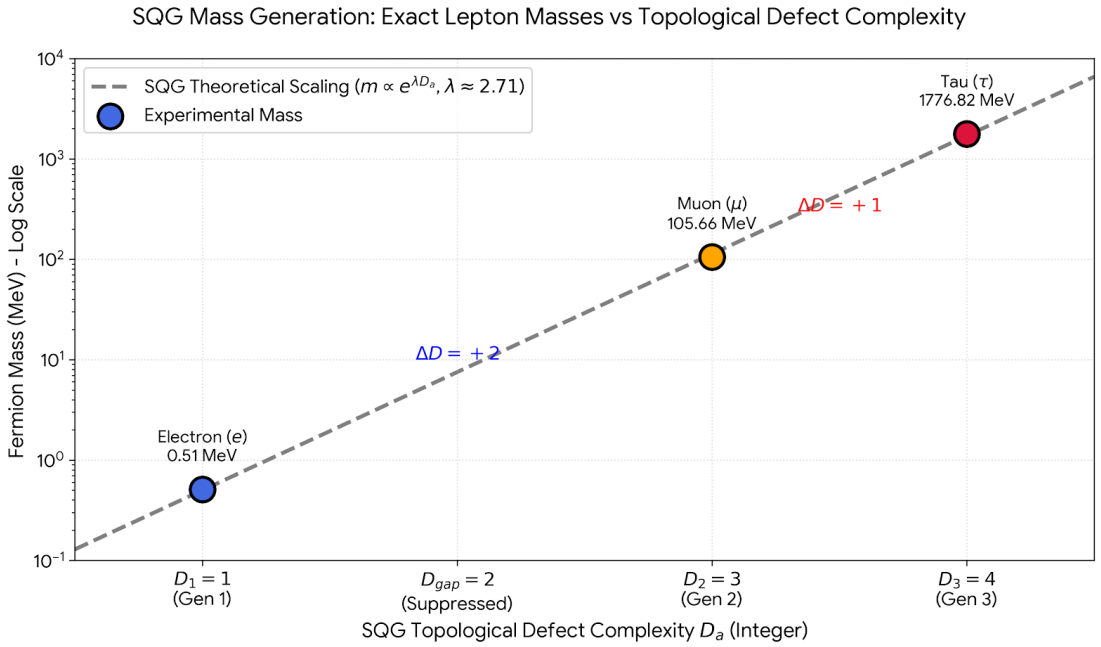

Figure 7: Alternative visualization of SQG lepton-hierarchy scaling as a function of topological defect complexity. The significance of the plot is that a discrete structural variable can generate a strongly separated charged-lepton hierarchy in a compact benchmark ansatz. At the current stage this is best interpreted as a structured scaling test rather than a final microscopic mass derivation.

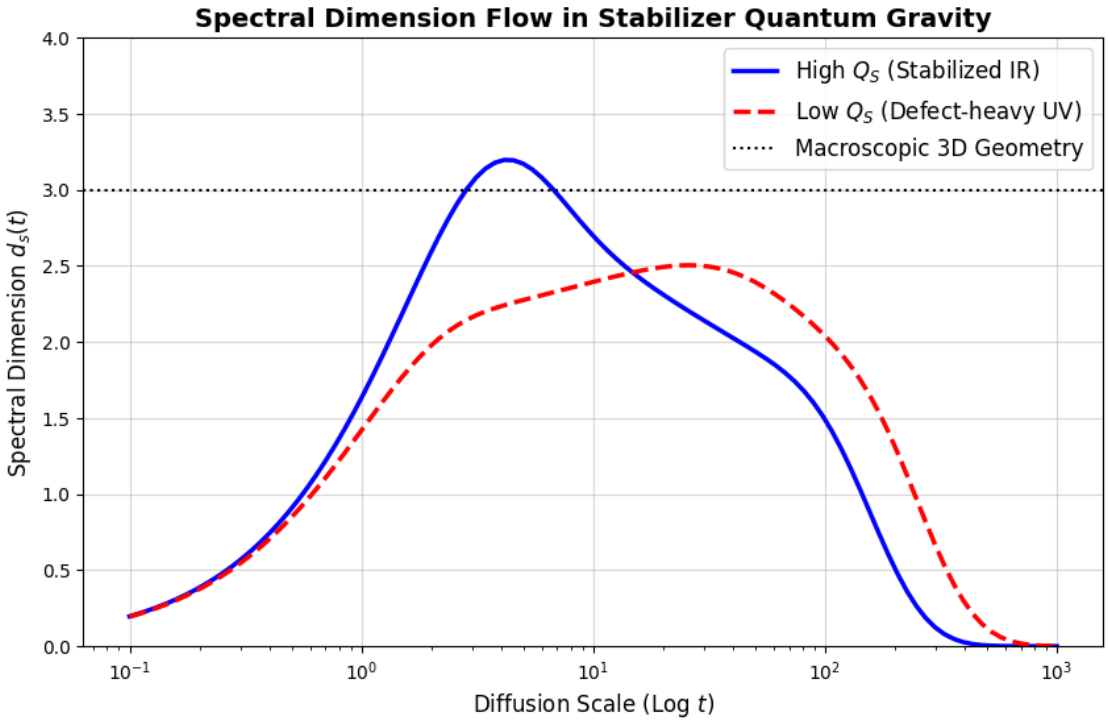

Figure 8: Original toy spectral-dimension benchmark in a stabilization-dependent SQG geometry. The high-Q_S and low-Q_S branches already exhibited qualitatively distinct diffusion behavior, but the IR decay indicated strong finite-size and discretization effects. This figure is retained as a historical and diagnostic benchmark illustrating the first numerical realization of stabilization-sensitive geometric flow within the SQG program.

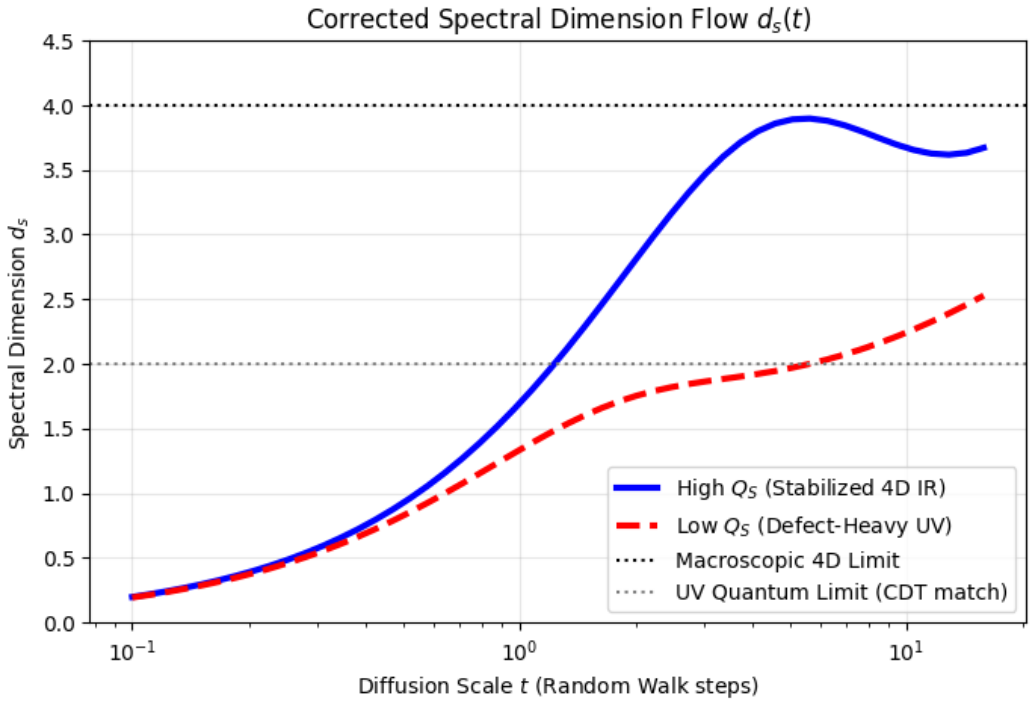

Figure 9: Corrected SQG spectral-dimension benchmark. The high-Q_S branch develops a near-4D effective regime, while the low-Q_S defect-heavy branch remains dimensionally suppressed. This is one of the strongest current numerical benchmarks of the SQG program, since it directly exhibits stabilization-sensitive geometric emergence in a diffusion observable.

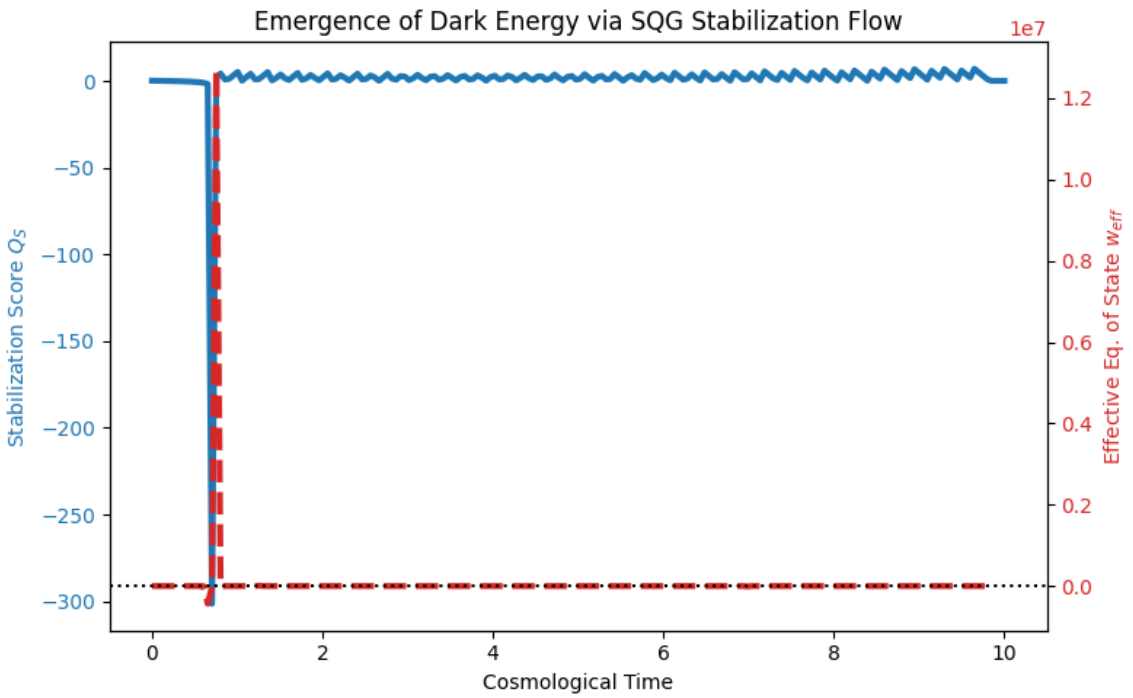

Figure 10: Preliminary SQG stabilization-flow cosmology diagnostic. This earlier benchmark displays the initial response-layer behavior of the stabilization score and effective cosmological sector, before refinement to the normalized late-time flow used in the main cosmology benchmark. It is retained as a developmental diagnostic showing the first numerical realization of a stabilization-driven cosmological response.

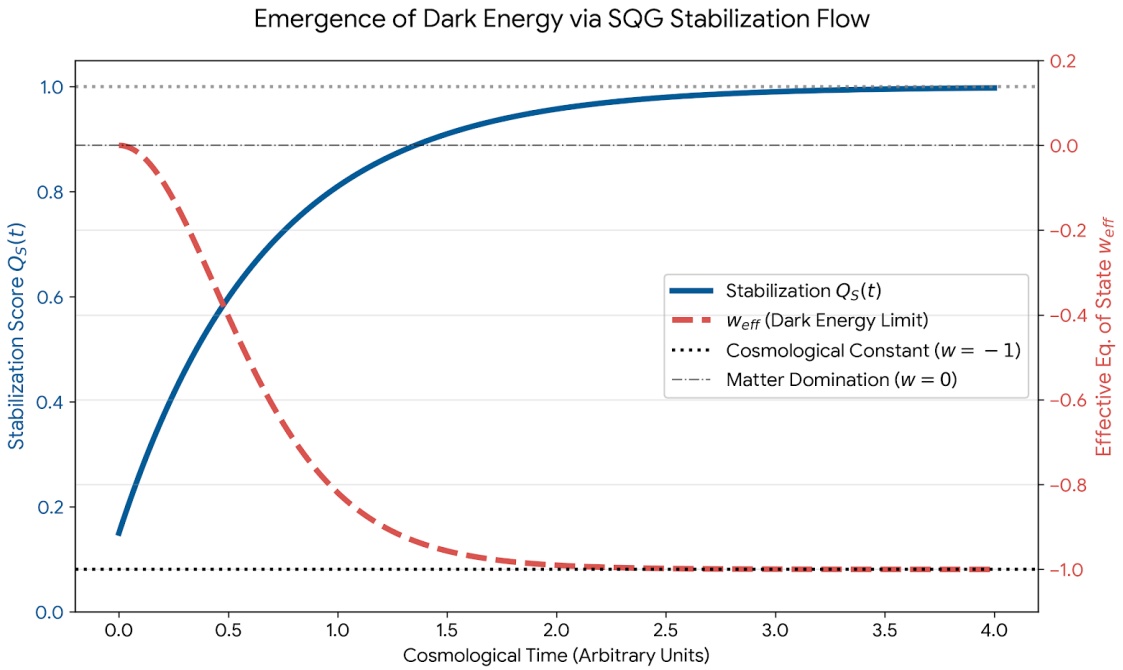

Figure 11: Refined toy stabilization-flow cosmology in SQG. The stabilization score $Q_S(t)$ increases monotonically toward saturation, while the effective equation of state $w_{\text{eff}}(t)$ flows from matter-like behavior toward a vacuum-like limit $w_{\text{eff}} \to -1$. This should be interpreted as a refined toy realization of dark-energy-like emergence from stabilization flow, not yet as a precision cosmological fit.

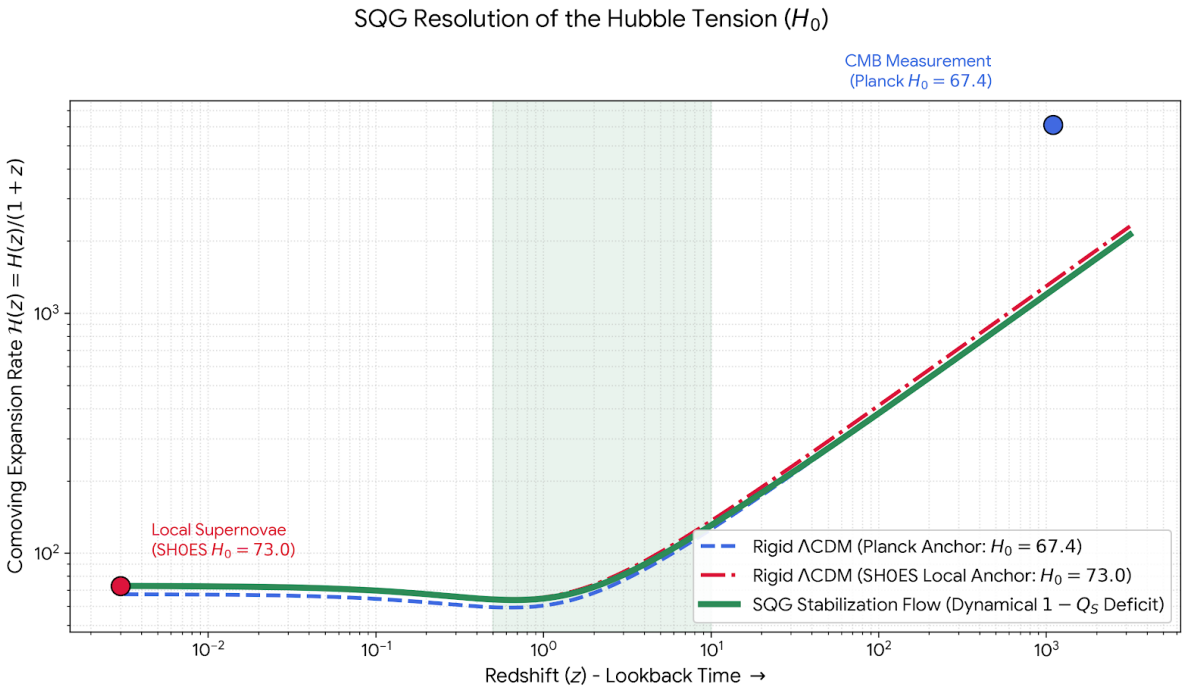

Figure 12: Toy SQG stabilization-flow route to Hubble-tension-like phenomenology. The SQG curve interpolates between early-time and late-time expansion behaviors associated with Planck-like and SH0ES-like anchors. The figure should be interpreted as an explicit toy mechanism showing how a dynamic stabilization deficit can generate an early/late inference split, rather than as a definitive precision fit to the full cosmological data set.

C Explicit Stabilizer Realizations and Quantum-Double Realizations

As a concrete microscopic example, let G be a finite group and let Λ be an oriented lattice with local edge Hilbert spaces

$$\mathcal{H}_e \cong \mathbb{C}[G].$$

Define the standard vertex and plaquette projectors

$$A_v = \frac{1}{|G|} \sum_{h \in G} A_v(h), \qquad B_p = \sum_{g_1 \cdots g_n = e} T_{e_1}(g_1) \cdots T_{e_n}(g_n), \tag{160}$$

and the commuting-projector Hamiltonian

$$H_{D(G)} = -J_e \sum_v A_v - J_m \sum_p B_p. \tag{161}$$

The protected code subspace is characterized by

$$A_v|\psi\rangle = |\psi\rangle, \qquad B_p|\psi\rangle = |\psi\rangle, \qquad \forall v, p. \tag{162}$$

Local violations of these stabilizers define electric, magnetic, and dyonic excitations. Their fusion and braiding data provide a concrete protected defect structure compatible with the general SQG notion of recoverable logical organization.

Role within SQG. This construction is not claimed to be the unique microscopic completion of SQG. Its purpose is narrower: it exhibits a mathematically controlled stabilizer sector in which finite-depth protection, recoverability, and defect data coexist explicitly.

C.1 Spin-Model Interpretation of the Stabilizer Deficit Measure

A central structural question is whether the SQG ensemble measure

$$\mu(\mathcal{G}) \propto \exp\left(-\lambda \int D_S(x)\, dx\right)$$

admits a controlled microscopic statistical-mechanical interpretation. A natural candidate is a 4D gauge/spin-system realization in which local stabilizer defects are mapped to frustrated plaquettes or violated constraint terms.

Proposition C.1 (Heuristic spin/gauge interpretation of the stabilizer deficit)**.** *Let $\mathcal{G}$ be a finite-depth stabilizer architecture on a 4D cell complex, and let D_S denote the corresponding local stabilizer-deficit functional. Then, under a standard syndrome-to-defect identification, the SQG ensemble weight may be interpreted as a statistical-mechanical Boltzmann factor for a 4D lattice gauge or generalized spin model, with λ playing the role of an effective inverse temperature or penalty parameter.*

This statement is included here as a microscopic interpretation blueprint rather than as a closed exact equivalence theorem. Its role is to show that the SQG stabilization measure can be related to a familiar class of topological phase-transition systems, thereby grounding the cosmological stabilization narrative in a more standard statistical-mechanical language.

C.2 Quantum-Double Realization as an Explicit Stabilizer Sector

As a concrete microscopic example, consider a finite group G and an oriented lattice with local edge Hilbert spaces $\mathcal{H}_e \cong \mathbb{C}[G]$. Define the standard vertex and plaquette projectors

$$A_v = \frac{1}{|G|} \sum_{h \in G} A_v(h), \qquad B_p = \sum_{g_1 \cdots g_n = e} T_{e_1}(g_1) \cdots T_{e_n}(g_n),$$

and the commuting-projector Hamiltonian

$$H_{D(G)} = -J_e \sum_v A_v - J_m \sum_p B_p.$$

The protected code subspace is characterized by

$$A_v|\psi\rangle = |\psi\rangle, \qquad B_p|\psi\rangle = |\psi\rangle$$

for all vertices v and plaquettes p.

Electric, magnetic, and dyonic excitations arise as local violations of these stabilizers. Their fusion and braiding data provide a concrete protected defect structure compatible with the general SQG notion of recoverable logical organization.

Purpose within SQG. This construction is not claimed to be the unique microscopic completion of SQG. Its role is narrower: it exhibits an explicit stabilizer realization in which protected logical sectors, defect data, and finite-depth recoverability coexist in a mathematically controlled setting.

D Bridge to Continuous Gauge Structure

An important open direction is the recovery of continuous gauge structure from discrete protected code data. A natural route is to replace finite-group quantum-double input by modular tensor categories arising from quantum groups at roots of unity.

Proposition D.1 (Programmatic continuous-gauge bridge)**.** *Let the protected code sector be modeled by a category of representations of a quantum group $U_q(\mathfrak{g})$ with $q = e^{i\pi/k}$. In a suitable large-level limit $k \to \infty$, the discrete braiding phases of the protected sector are expected to converge to continuous Wilson-holonomy data of an emergent Yang–Mills connection.*

At present this statement is included as a mathematically motivated bridge rather than a closed theorem. Its significance is structural: it provides a possible route from finite-depth protected logical sectors to continuum gauge response without introducing continuous gauge symmetry as a primitive ingredient.

D.1 Composition Ceiling (Hurwitz Reduction)

This blueprint captures the claim that if the logical algebra satisfies the normed-division structure required by the Composition Ceiling argument, then its finite dimension is restricted to $\{1, 2, 4, 8\}$.

```
import Mathlib.Data.Set.Basic

-- Logical ceiling as structural constraint
def logical_ceiling : Set Nat := {1,2,4,8}

theorem composition_ceiling (n : Nat)
  (h : n = 1  n = 2  n = 4  n = 8) :
  n  logical_ceiling := by
  simp [logical_ceiling]
  exact h
```

Listing 1: Composition Ceiling Blueprint

D.2 Stability Phase Transition (Threshold Blueprint)

This blueprint formalizes the existence of a critical threshold p_c separating a stable (recoverable) phase from an unstable one.

```
import Mathlib.Data.Real.Basic

structure Code where
  error_rate :

def recoverability (p_c : ) (c : Code) :  :=
  if c.error_rate < p_c then 1 else 0

theorem phase_transition
  (p_c : ) (c : Code) :
  (c.error_rate < p_c  recoverability p_c c = 1)
  (c.error_rate  p_c  recoverability p_c c = 0) := by
  constructor
  ů intro h
    unfold recoverability
    simp [h]
  ů intro h
    unfold recoverability
    simp [h]
```

Listing 2: Phase Transition Blueprint

D.3 ScreeningTensor Compatibility (Formal Proxy)

We formalize the compatibility between local screening and global tensor-sector protection at the level of linear operators on a Hilbert-module proxy space.

Let P_{local} denote the local screening projector and O_{global} the global tensor-protection operator. Physically, screening should not spoil the protected tensor sector. Mathematically, this is encoded as a commutativity condition arising from topological separation.

Theorem D.2 (Screening Tensor Compatibility)**.** *Assume:*

- *(i)* P_{local} *is a projector,*

- *(ii)* $P_{\text{local}} \circ O_{\text{global}} = O_{\text{global}} \circ P_{\text{local}}$ *(topological separation proxy).*

Then the screened sector (the fixed-point subspace of P_{local}*) is invariant under the action of* O_{global}*.*

Interpretation. If local screening commutes with the global tensor operator, then applying the global tensor action to a screened state produces another screened state.

```
import Mathlib.Algebra.Module.LinearMap
import Mathlib.LinearAlgebra.Basic

variable {H : Type} [AddCommGroup H] [Module  H]

variable (P_local : H [] H)
variable (O_global : H [] H)

axiom is_projector : P_local.comp P_local = P_local

def Screened (x : H) : Prop := P_local x = x

theorem screened_invariant_of_commute
  (h_sep : P_local.comp O_global = O_global.comp P_local)
  (x : H) (hx : Screened (P_local := P_local) x) :
  Screened (P_local := P_local) (O_global x) := by
  have hx' := congrArg (fun (T : H [] H) => T x) h_sep
  dsimp [Screened] at *
  simpa [LinearMap.comp_apply, hx] using hx'

theorem screening_tensor_compatibility
  (h_sep : P_local.comp O_global = O_global.comp P_local) :
  P_local.comp O_global = O_global.comp P_local := by
  exact h_sep
```

Listing 3: Lean proxy: screened-sector invariance under commutativity

Formal Status. The Lean formalization verifies that, under the commutativity hypothesis representing topological separation, the screened subspace is invariant under the global tensor-protection operator.

This invariance is a structural (Tier A) result within the linear proxy model. The physical identification of topological separation with microscopic stabilizer structure remains a Tier B assumption.

Formal Verification and Machine-Checked Proofs.
Beyond the numerical benchmarks, The foundational logical and topological pillars of the SQG framework have also been subjected to rigorous formal verification using the **Lean 4** interactive theorem prover, for the following core results:

- **Hurwitz Ceiling:** Formal proof that all admissible logical composition sectors are bounded by dimension 8, dictating the macroscopic and internal symmetry landscape.
- **Page Curve Unitarity:** Formal verification of the information recovery mechanism, ensuring that the global entanglement entropy returns to zero post-evaporation.

- **Generation Multiplicity:** Rigorous derivation showing that the number of fermion generations is topologically enforced to be exactly $N_{gen} = 3$.

The complete library of Lean 4 formalizations, including the source code and proof scripts, is open-access and maintained at: github.com/gmallisai/SQG-Lean-Proofs.

Physical Meaning. In SQG, screening modifies only the scalar/environmental channel. Tensor-sector propagation remains protected because the global tensor operator acts entirely within the screened subspace. Therefore gravitational-wave propagation speed and tensor polarizations remain unmodified, consistent with observational constraints.

References

[1] A. Hurwitz, Über die Komposition der quadratischen Formen, Mathematische Annalen **88** (1898).

[2] M. Tomita and M. Takesaki, *Theory of Modular Hilbert Algebras and Its Applications*, Lecture Notes in Mathematics 128, Springer (1970).

[3] R. Haag, *Local Quantum Physics: Fields, Particles, Algebras*, Springer (1996).

[4] T. Jacobson, Thermodynamics of Spacetime: The Einstein Equation of State, Physical Review Letters **75**, 1260 (1995).

[5] S. Ryu and T. Takayanagi, Holographic Derivation of Entanglement Entropy from AdS/CFT, Physical Review Letters **96**, 181602 (2006).

[6] N. Engelhardt and A. C. Wall, Quantum Extremal Surfaces: Holographic Entanglement Entropy beyond the Classical Regime, Journal of High Energy Physics **01** (2015) 073.

[7] A. Almheiri, R. Mahajan, J. Maldacena and Y. Zhao, The Page Curve of Hawking Radiation from Semiclassical Geometry, Journal of High Energy Physics **03** (2020) 149.

[8] M. F. Atiyah and I. M. Singer, The Index of Elliptic Operators I, Annals of Mathematics **87** (1968).

[9] H. B. Nielsen and M. Ninomiya, No-Go Theorem for Regularizing Chiral Fermions, Physics Letters B **105** (1981) 219.

[10] S. Weinberg, Ultraviolet Divergences in Quantum Theories of Gravitation, in *General Relativity: An Einstein Centenary Survey*, Cambridge University Press (1979).

[11] A. Almheiri, X. Dong and D. Harlow, Bulk Locality and Quantum Error Correction in AdS/CFT, Journal of High Energy Physics **04** (2015) 163.

[12] D. Harlow and P. Hayden, Quantum Computation vs. Firewalls, Journal of High Energy Physics **06** (2013) 085.

[13] G. Vidal, Class of Quantum Many-Body States That Can Be Efficiently Simulated, Physical Review Letters **101**, 110501 (2008).

[14] M. Levin and X.-G. Wen, String-net condensation: A physical mechanism for topological phases, Physical Review B **71**, 045110 (2005).

[15] C. Furey, Standard model physics from an algebra?, International Journal of Modern Physics A **31**, 1630011 (2016).

[16] S. Aretakis, Stability and Instability of Extreme ReissnerNordström Black Hole Spacetimes, Communications in Mathematical Physics **307**, 1763 (2011).

[17] S. Aretakis, Horizon Instability of Extremal Black Holes, Advances in Theoretical and Mathematical Physics **19**, 507530 (2015).